International Code for Phytolith Nomenclature (ICPN) 2.0

International Committee for Phytolith Taxonomy (ICPT)

(Katharina Neumann, Caroline Strömberg, Terry Ball,

Rosa Maria Albert, Luc Vrydaghs, Linda Scott Cummings)

Supplementary Information: Morphotype Descriptions

ACUTE BULBOSUS

Code: ACU_BUL

ICPN 1.0: Acicular hair cell. Unciform hair cell

Rationale for naming: Because the taxonomic occurrence and anatomical origin of this type cannot always be certain, it is given a morphological name. The morphotype includes a morphological spectrum that is characterized by their acute apex and more bulbous antapex.

Description: Unarticulated, solid body with a generally narrower, acute part (referred to as the apex), and another, wider part (referred to as the antapex). The antapex is hemi-spheroidal (rounded), truncated hemispheroidal, or has a near-parallelepipedal to fusiform shape with more or less pointed ends. The apex can be straight or curved, with a sharp or rounded tip. It often forms an angle of less than 90^{o} with the long axis of the antapex, resulting in a markedly asymmetrical, roughly triangular shape in side view. The body overall consists of granular or homogenous silica, typically obscure and/or maculose. The antapex can have multiple simple or dendritic processes covering part of its surface.

Size: Generally ~25-100 µm long (tip of apex to antapex), but can be longer (>100 µm).

Anatomical origin and taxonomic occurrence: In grasses, ACUTE BULBOSUS represents infilling of the interior (cell lumen) of a hair cell (mainly "prickle-hairs" of Metcalfe, 1960). In other taxa, it is not always clear whether ACUTE BULBOSUS reflects infilling of an epidermal appendage such as a trichome, or a cell type from another tissue.

ACUTE BULBOSUS is found in many grasses (e.g., Brown, 1984; Piperno, 1988, 2006; Runge, 1998, 1999), and has also been reported from sedges (Piperno, 1983, 1988; Strömberg, 2003), and in low frequencies in *Equisetum*, *Selaginella*, certain dicotyledons, and a palm (Strömberg, 2003; Piperno, 1988, Fig. 46).

Discussion and interpretation: ACUTE BULBOSUS is often found associated with silicified trichome cell walls, consisting of one or multiple separate layers of smooth, opaline silica loosely surrounding the apex of ACUTE BULBOSUS. These silicified cell walls rarely preserve in soil/sediment or archaeological phytolith assemblages; however, when they do, they can be more diagnostic than ACUTE BULBOSUS by itself (e.g., grasses tend to have hair cells with two cell layers; Hayward and Parry, 1975). For this reason, we prefer to treat the silicified cell walls (or the combination of cell walls and ACUTE BULBOSUS) as a separate morphotype (see Strömberg, 2003).

ACUTE BULBOSUS is commonly found and abundantly produced in grasses; it is therefore frequently used as diagnostic of grasses (Alexandre *et al.*, 1997; Barboni *et al.*, 2007; Zucol *et al.*, 2010).

Synonyms: Morphotype class Aculeolita (in part) (Bertoldi de Pomar, 1975, Plate IV, Figs. 5, 8, 9, 14, 15). Trichomes, short and long (types IIA3, IIC3) (Brown, 1984, Fig. 1). Non-segmented hair phytolith (Piperno, 1988, Fig. 46). Point-shaped phytolith (Twiss, 1992, Fig. 6.1). Small prickle (Kaplan *et al.*, 1992; types IIa1, Fig. 8.9; type IIb2, Fig 8.15). Silicified prickle base from Poaceae (Runge, 1998, Plate V.8, Type G3). Spindle-shaped body (trichome filling) (Tri-8) (Strömberg, 2003, Fig. 4.10d). Simple trichome (Strömberg, 2004). Silicified trichome (ht) and silicified hair or hair base (hh) (Blinnikov, 2005, Plate I.14-15 and Fig. 2. 14-15). Prickle hairs, hook hairs, macrohairs (Fernandez-Honaine *et al.*, 2006, Fig. 2E-G). Point-shaped (Ps) types Ps01-09 (Zucol *et al.*, 2010, Figs. 22.4E, 22.7.1-9). Acicular type (Aci1) (Novello and Barboni, 2015, Plate 1).

Illustrations: Fig. 1A-M.

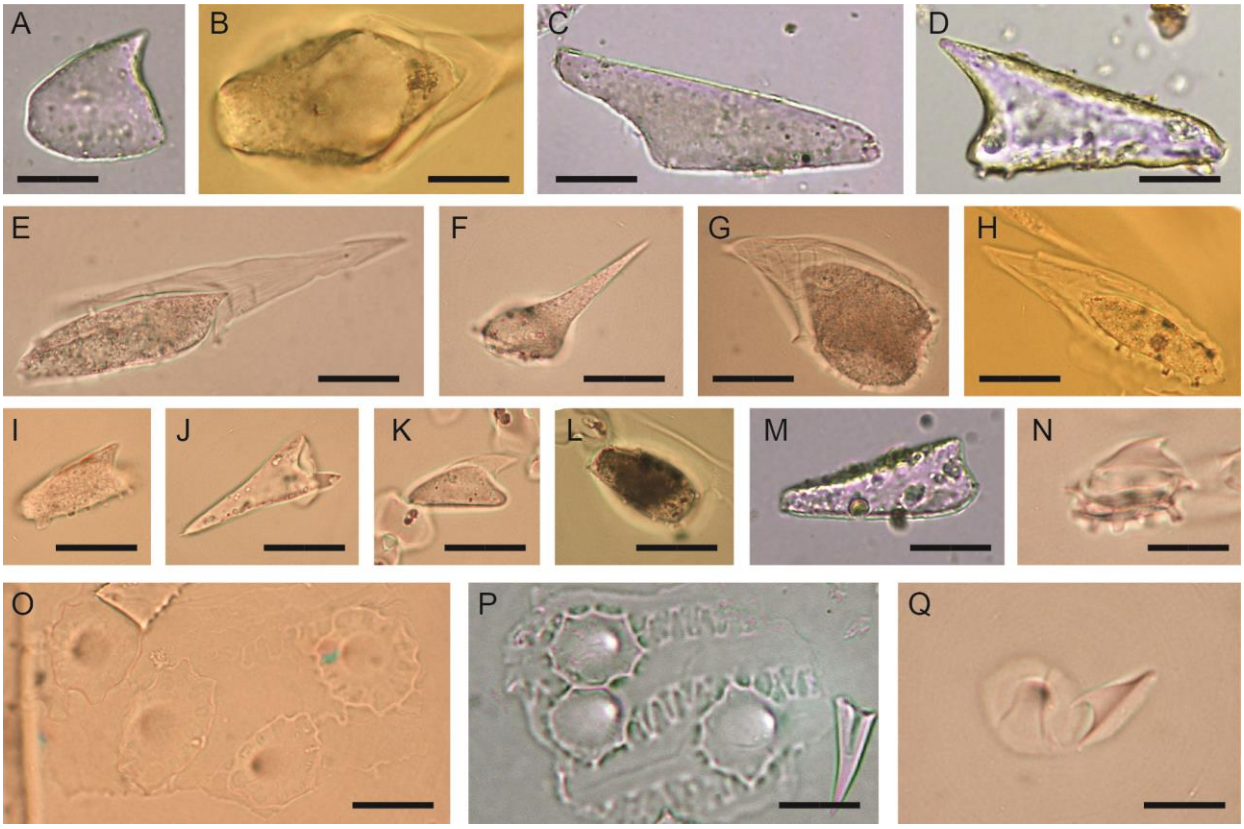

FIG. 1. ACUTE BULBOSUS and PAPILLATE. (A-M) ACUTE BULBOSUS, side view unless otherwise noted, (A) Archaeological sample, Pondoland C4 site (South Africa), (B) *Carex mendocinensis* (Cyperaceae), leaf, antapex view (UCMP 399335), (C) Archaeological sample, Pondoland C4 site (South Africa), (D) Archaeological sample, Roman site of Pollentia (Mallorca, Spain), (E) *Deschampsia caespitosa* (Poaceae), spikelet (UCMP 399352), (F) *Triticum aestivum* (Poaceae), spikelet (UCMP 399375), (G) *Calamagrostis ophiditis* (Poaceae), leaf (UCMP 399344), (H) *Aristida purpurea* var. *wrightii* (Poaceae), leaf (UCMP 399340), (I) *Dactylis glomerata* ssp. *Hispanica* (Poaceae), leaf (UCMP 399348), (J-L) *Glyceria striata* var. *striata* (Poaceae), leaf (UCMP 399356), (L) in apex view, (M) Archaeological sample, Pondoland C4 site (South Africa), (N-Q) PAPILLATE, apex view unless otherwise noted, (N) *Dactylis glomerata* ssp. *Hispanica* (Poaceae), spikelet, side view (UCMP 399349), (O) *Triticum aestivum* (Poaceae), spikelet (UCMP 399375), (P) *Hordeum vulgare* (Poaceae), reproductive material, Israel Reference Collection, (Q) *Melica nitens* (Poaceae), spikelet, apex and side view (UCMP 399361). Authors: A, C-D, M, P: R.M. Albert and I. Esteban; B, E-L, N-O, Q. C.A.E. Strömberg. Scale = 20 µm, except in N, Q = 10 µm .

PAPILLATE

Code: PAP

Synonyms: ICPN 1.0: Papillae

Rationale for naming: This morphotype forms in, and takes the shape of, a specialized trichome, found primarily in the inflorescence of grasses, that has not been given a specific name in the anatomical literature (see e.g., Metcalfe, 1960; Parry and Smithson, 1966), hence we give it a morphological name.

The name PAPILLATE refers to the overall, nipple-like shape. The brevity of the name recognizes the importance of this morphotype within archaeobotany (see e.g., Rosen, 1992; Tubb *et al.*, 1993; Ball *et al.*, 1999).

Description: Circular to oval ("saucer-shaped", Parry and Smithson, 1966) plate (antapex) with a short, conical, blunt or pointy protrusion (apex) in the center where the plate is thickest. The protrusion points obliquely at an angle <90˚ with the plane of the plate. The plate is made up of smooth, homogeneous opaque material and ranges from being very thin and transparent to being thickened and (at higher magnification) laminated in cross section (with lamination parallel to the surface). In cases when the entire perimeter of the plate is silicified, its edges can be sinuate, sometimes with small circular holes/pits.

Size: Typically ~10-20 µm in diameter.

Anatomical origin and taxonomic occurrence: This morphotype results from the silicification of a short cell, specifically a modified prickle hair (e.g., Parry and Smithson, 1966; Hayward and Parry, 1980). The plate represents the silicification at or in the distal/outer cell wall and the branched sphere (see below) represents the infilled lumen of the short cell. The homology with other trichomes is indicated by the fact that in some samples the apex of the plate can be drawn out into a very sharp point, reminiscent of the apex of a "true" prickle hair (Parry and Smithson, 1966; Strömberg, 2003).

The morphotype is known from inflorescence bracts of grasses (Parry and Smithson, 1966; Kaufman *et al.*, 1972; Sangster *et al.*, 1983; Ball *et al.*, 1996; 1999; Piperno, 2006), although some authors have also reported them from grass culms and leaves (Brown, 1984; Ball *et al.*, 1993). The variations in size, density, and ornamentation of these morphotypes, as well as the quantity of small pits in the plate, have been used by some authors to differentiate between wild and domestic cereals and between wheat and barley (Rosen, 1992; Tubb *et al.*, 1993; Hodson *et al.*, 2001).

Discussion and interpretation: The plate is commonly preserved with a spheroidal or horizontally flattened circular body of solid, granulate to homogeneous silica, with thick, dendritic processes covering its surface (referred to as "round spiky opals" or "asteriform opals"; Parry and Smithson, 1966; Hayward and Parry, 1980; Piperno, 1988). PAPILLATE can also be found associated with ELONGATE SINUATE, ELONGATE DENTATE, and ELONGATE DENDRITIC. PAPILLATE can be somewhat similar to simple sedge-plates, but can be differentiated because the apex of PAPILLATE points at an oblique angle and is often offset from the center of the plate.

PAPILLATE are diagnostic of grasses, specifically grass inflorescences (e.g., Piperno, 2006).

Synonyms: Scutiform opal (Parry and Smithson, 1966, Plate 2, Figs. 18, 20-23, Plate 3, Figs. 24, 25). Variants 34 and 35 in the morphotype class Pileolita (Bertoldi de Pomar, 1971, Figure, p. 323). Papillae (Sangster *et al.*, 1983, Figs. 2-4). Trichomes, short, conical hook (types IIA1a, b) (Brown, 1984, Fig. 1). Small prickle (Kaplan *et al.*, 1992; types IIa1, Fig. 8.8; type IIa2, Fig. 8.10-11). Short, solid cones (Ollendorf, 1992, Fig. 5.2). Small prickle phytoliths (Ball *et al.*, 1993, Figs. 1, 6, 7, 13, 14). Grass inflorescence hook-shaped short cell (modified trichome) (Tri-12) (Strömberg, 2003, Fig. 4.10h). Point-shaped (Ps) type Ps10 (Zucol *et al.*, 2010, Fig. 22.7.10).

Illustrations: Fig. 1N-Q.

BLOCKY

Code: BLO

ICPN 1.0: Parallelepipedal bulliform cell

Rationale for naming: BLOCKY is very intuitive, commonly accepted term best describing phytoliths with ± parallelepipedal shapes that do not perfectly match a geometrical parallelepiped. "Parallelepipedal bulliform cell" of ICPN 1.0 should not be used because parallelepipedal bulliforms cannot be differentiated from other BLOCKY phytoliths unless identified in an anatomical context.

Description: BLOCKY encompasses compact, heavily built, solid phytoliths with length/width <2, and width and thickness roughly equal. In 3-D perspective the overall shape resembles a parallelepiped (a 6-faced parallelogram), although there can be more faces. The faces may be flat, slightly convex or concave. The edges of the faces are sharp or blunt. From a 2-D perspective some BLOCKY present four or more sides. Some BLOCKY have projections at the edges, ridges, facets or protrusions that may appear as dentate margins in certain views. They may also show slightly uneven or velloate edges corresponding to the intersection of formerly adjacent cells. Surfaces can be psilate, granulate, or columellate.

Size: 40-150 µm in length (varies greatly).

Anatomical origin and taxonomic occurrence: BLOCKY are very common in the leaves of Cyperaceae and Poaceae where they often represent bulliform and related, sub-epidermal cells (Esau, 1965, p.153). However, BLOCKY are also commonly found in other monocots, as well as in dicots and conifers (Strömberg, 2003). They may derive from parenchyma, sclerenchyma, and cork, but mostly their origin is currently unknown. For example, they have been found in the bark of various dicotyledonous trees from the Mediterranean (Albert, 2000; Tsartsidou *et al.*, 2007) and Africa (Collura and Neumann, 2017), and in *Artemisia* (Blinnikov *et al.*, 2002), as well as in the needles of several gymnosperms (e.g., Pinaceae, Cupressaceae, Taxaceae).

Discussion and interpretation: Due to the wide distribution in different plants, the diagnostic value of BLOCKY is low. When identified in Poaceae and Cyperaceae in an anatomical context, they can be interpreted as bulliform cells. BLOCKY with columellate surfaces are likely sclereids, and have not yet been reported in grasses. BLOCKY with bordered pit impressions are classified as TRACHEARY BORDERED (see below).

Synonyms: Rectangles/Squares plus some bulliforms cells (Mulholland and Rapp, 1992). Blocky polyhedron (Bozarth, 1993, Fig. 2a). Polyhedral [Sase and Hosono, 2001, Fig. 1, Last Glacial Phytolith (14-15); Last Interglacial Phytoliths (12-13)]. Rounded blocky (Blinnikov *et al.*, 2002, Fig. 3.16). Sculptured blocky (Blinnikov *et al.*, 2002, Fig. 3.17). Blocky bodies (Blo), in part contained in Rectangular plates (Blo-1), Thickened rectangular plate (Blo-2), Faceted rectangular plate (Blo-3), Thick polyhedral plate (Blo-4), *Chamaerops* blocky polyhedron (Blo-5), Blocky polyhedron (Blo-6), Thick trapezoidal rectangle with knobs (Blo-7), Sulcate, facted 3D polyhedron (Blo-8), Bulliform A: radiator-shaped body (Blo-9) (Strömberg, 2003, Fig 4.15, a-j). Blocky types subdivided between cubic, hexagonal, parallelepipeds and other types (Barboni *et al.*, 2010, Fig. 4. 25-33). Blocky polyhedral (An, 2016, Fig. 1a-d). Cubic (An 2016, Fig. 1a-d). Blocky, Blocky velloate (PhytCore: www.PhytCore.org).

Illustrations: Fig. 2.

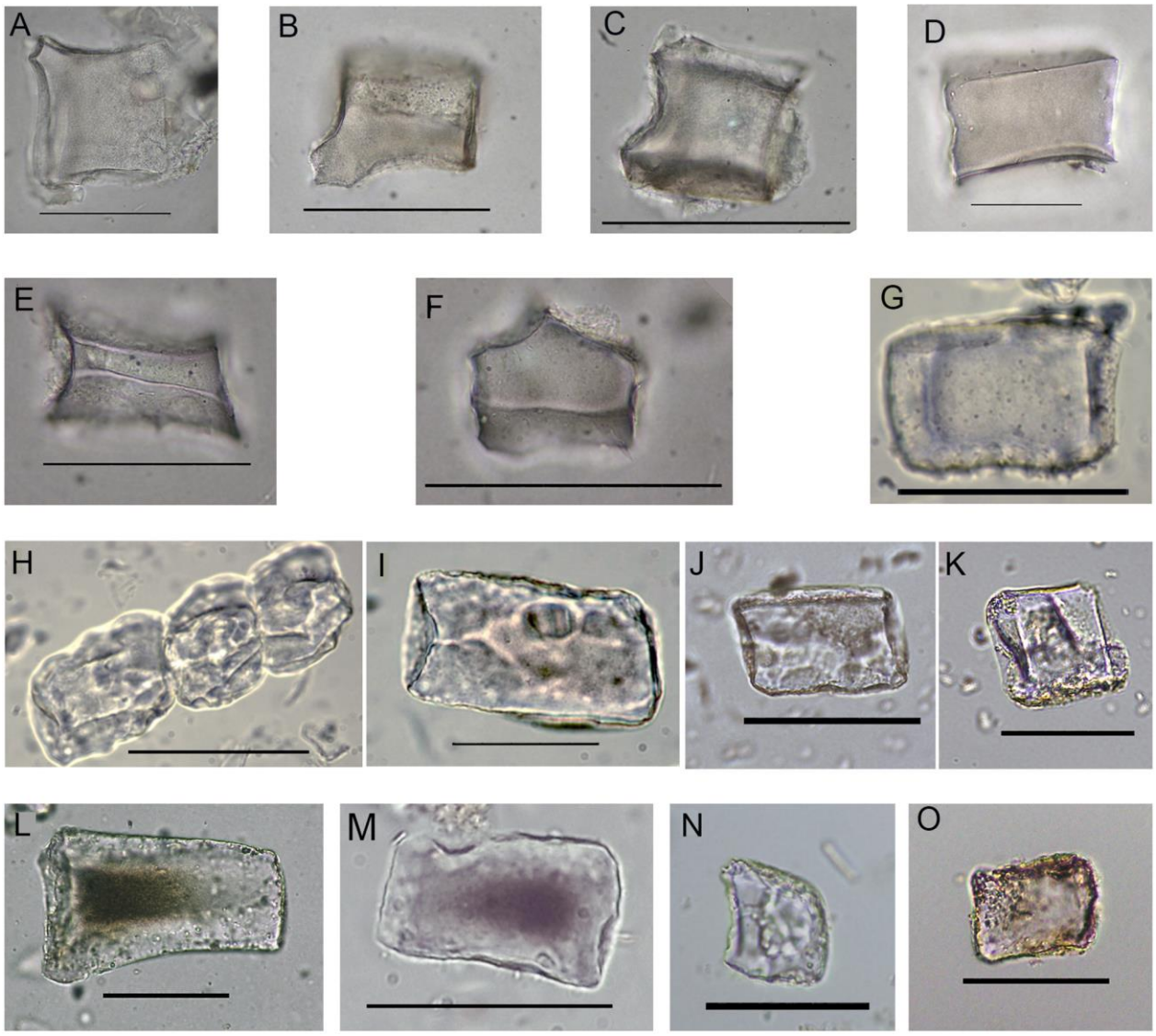

FIG. 2. BLOCKY. (A-H) Modern plant reference material, (A-C) *Pinus resinosa* (Pinaceae), bark, (D-F) *Pinus strobus* (Pinaceae), bark, (G-H) *Sarcophrynium priogonium* (Marantaceae), leaf (PHV 179), (I) Sediment sample from Cameroon, (J) Modern surface soil sample from Serengeti National Park (Tanzania), (K) Modern surface soil sample from Lake Masek (Tanzania), (L) Ancient soil from Pondoland (South Africa), (M) Archaeological sample, Pinnacle Point 13A, (N-O) Archaeological samples, Olduvai Gorge (Tanzania). Scale: A-F: 100 µm; G-O: 50 µm. Authors: A-F: C. Yost; G-I: K. Neumann; J-O: R.M. Albert, I. Esteban and A. Rodríguez-Cintas.

BULLIFORM FLABELLATE

Code: BUL_FLA

ICPN 1.0: Cuneiform bulliform cell

Rationale for naming: An anatomical name is justified for this morphotype because it can be unequivocally attributed to the intracellular silicification of bulliform cells of Poaceae and Cyperaceae (Esau 1965; Metcalfe 1960, p. 684-685, 1971). Flabellate specifies the general morphotype shape.

Description: Heavily built, solid phytolith, tabular, flabellate. The lower part of this fan-shaped morphotype is markedly narrower than the upper part. The outline of the upper part is generally convex and may be facetate. In some cases, the top of the upper part can be truncated, resulting in a flat to concave face. The sides of the lower part can be straight to concave. The outline of the base can be straight to typically convex. The phytolith is often symmetrical along an axis from top to base [vertical length (VL); Fujiwara, 1993], but can also be asymmetrical. The surface is typically psilate. For definitions of the different lengths used to measure this morphotype see also Fujiwara (1993).

Size: Long axis or vertical length (VL) from top to base 40-200 µm.

Anatomical origin and taxonomic occurrence: BULLIFORM FLABELLATE are large, specialized epidermal cells that occur in longitudinal rows in the furrows of the leaf surface in Poaceae and Cyperaceae (Esau, 1965; Metcalfe, 1960, 1971). The facets on the outline of the upper part represent the impressions of adjacent cells. It is generally assumed that bulliform cells facilitate leaf rolling or folding by decreased turgor pressure as plant water potential decreases (Esau, 1965: p. 153).

Discussion and interpretation: The morphological characteristics of the BULLIFORM FLABELLATE make them easily recognizable and attributable to Poaceae and Cyperaceae. Nevertheless not all bulliform phytoliths produced by Poaceae and Cyperaceae have the distinctive flabellate shape of this morphotype, but rather would be classified as BLOCKY. A high production of silicified bulliform cells is usually related to high water availability (Sangster and Parry, 1969; Rosen and Weiner, 1994; Fisher *et al.*, 2013). Other studies (Bremond *et al*., 2005; Issaharou-Matchi *et al*., 2016) also point to the fact that water stress and increased evapotranspiration increase bulliform production.

A study by Pearsall *et al.* (1995) used the size and shape of BULLIFORM FLABELLATE to identify rice, and others have analyzed bulliform morphotypes in attempts to differentiate between wild and domesticated rice (e.g. Huan *et al.*, 2015).

Synonyms: Bulliform cells, Category 50 (Pearsall and Dinan, 1992, 41, Fig. 3.1A). Motor cell silica body (Fujiwara, 1993, Figs. 2-6, 8-10, 15, 18). Keystone bulliform cells (Pearsall *et al.*, 1995). Fan-shaped [Sase and Hosono, 2001, Fig. 1, Holocene phytoliths (1-2), Last Glacial Phytoliths (8-9), Last Interglacial Phytoliths (1, 14-17)]. Grass Bulliform phytolith and Bulliform (Piperno, 2006, Figs. 2.3a, 3.9c). Cuneiform Bulliform (Yost and Blinnikov, 2011, Fig. 3D, 8O, 9L). Bulliform flabellate (PhytCore: www.phytcore.org).

Illustrations: Fig. 3.

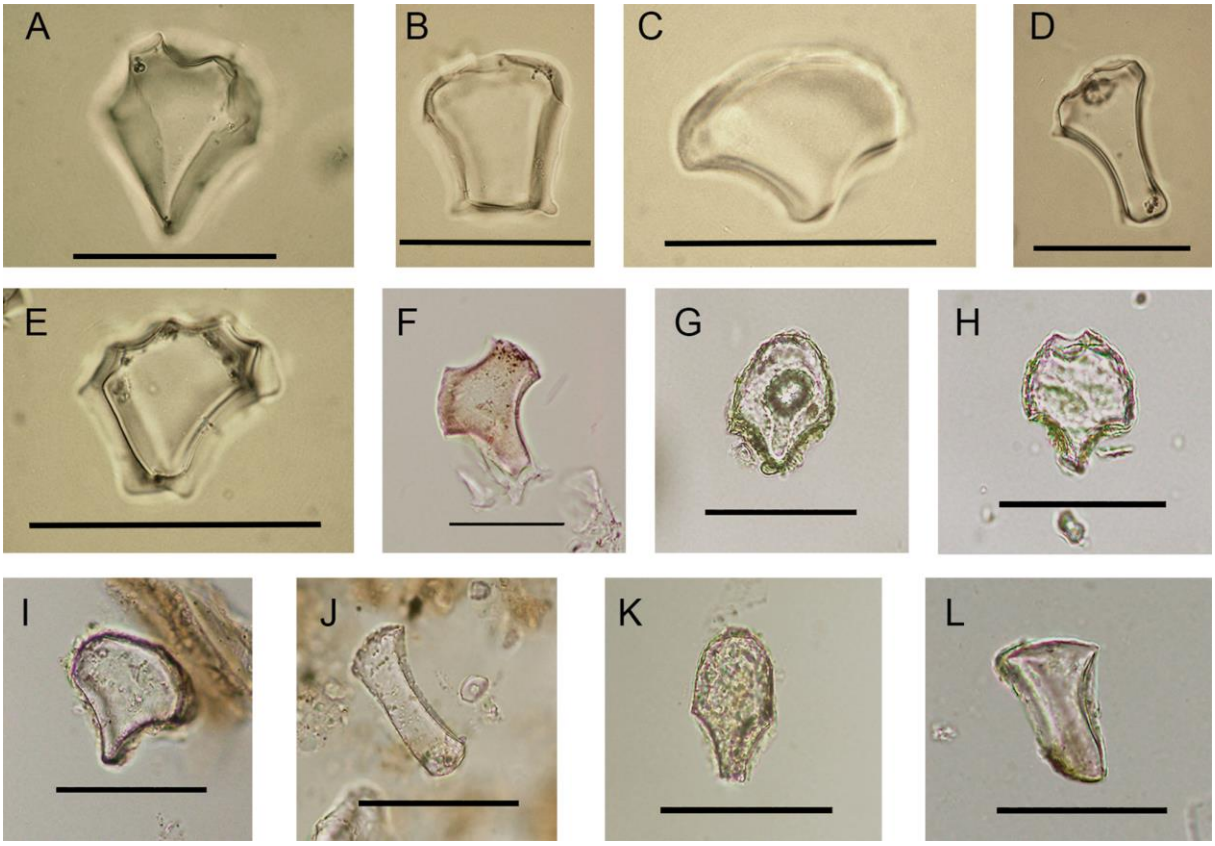

FIG. 3. BULLIFORM FLABELLATE. (A-F) Modern Plant Reference material. (A, D-E) *Otatea acuminata* ssp. *aztecorum* (Poaceae), leaf (UCMP 399367), (B) *Streptogyna gerontogaea* (Poaceae), leaf (UCMP 399373), (C) *Eragrostis ferruginea* (Poaceae), leaf (UCMP 399353), (F) *Sporobolus consumilis* (Poaceae), leaf (UB_OLD_RC02_077), (G-H) Modern surface sediment samples from Lake Manyara (Tanzania), below *Aristida triornis* (Poaceae), (I-L) Archaeological samples, (I-K) Archaeological samples, Olduvai Gorge (Tanzania), (L) Archaeological sample, Llanos de Moxos (Bolivia). Scale: A-C; F-L= 50 µm; D-E: 35 µm. Authors: A-E: C.A.E. Strömberg; F-K: R.M. Albert; L: I. Esteban.

ELONGATE ENTIRE

Code: ELO_ENT

Rationale for naming: ELONGATE ENTIRE is widely produced among modern land plants; thus, a taxonomic name is not appropriate. Because their anatomical origin is also not always known, it is necessary to give them a morphological name. The name refers to the most conspicuous character of the morphotype: its elongated shape and its entire margins.

Description: ELONGATE ENTIRE has an overall rectilinear 2D outline and highly variable sizes. Slightly arcuate elongated phytoliths with more or less parallel long sides are also included. L:W is characteristically ≥2. The margins are smooth, without distinct projections or indentations, but sometimes slightly uneven or velloate, corresponding to the inter-section of formerly adjacent cells. Ends can be concave, convex, straight, rounded or tapering. Their transverse section can range from angular (e.g., rectangular) or circular to oblong in shape. Thickness can range from thinly tabular to robustly thick. Their surface texture can range from psilate to granulate. Often observed

as single cells, but also occurring articulated, arranged in parallel or longitudinal consecutive patterns.

Size: Length 20-700 µm.

Anatomical origin and taxonomic occurrence: ELONGATE ENTIRE can result from the silicification of cells within different plant tissues and organs, such as epidermis, subepidermal tissue, parenchyma and sclerenchyma. ELONGATE ENTIRE have been reported from lycophytes, conifers, monocotyledons, and eudicotyledons (Strömberg, 2003). They are very common in the epidermis of monocotyledons, especially in Poaceae leaves and culms where, together with ELONGATE SINUATE and ELONGATE DENTATE, they constitute the majority of the long cells in the intercostal zones. [Note that the anatomical term "long cell" also applies for other non-GSSCP morphotypes with a L:W ratio of ≤2 in the epidermis of the grass leaf (Metcalfe, 1960: XX, 669, Fig. V)].

Discussion and interpretation: The L:W characteristically ≥2 distinguishes the morphotype from BLOCKY which has a L:W of <2. Transitional forms with ELONGATE SINUATE, ELONGATE DENTATE and ELONGATE DENDRITIC occur.

ELONGATE ENTIRE is one of the most commonly produced phytoliths morphotypes among land plant taxa, but because of its wide occurrence, it is often omitted from the description of phytolith assemblages in modern plants. Its taxonomic diagnostic value is low. According to their cross section (triangular, quadrilateral or circular) as well as their thickness (thin, thick), ELONGATE ENTIRE can be further divided into various sub-types: trihedral (triangular transverse section), cylindrical (circular to oblong transverse section), parallelepipedal (thick quadrilateral transverse section), or tabular (thin quadrilateral transverse section). The anatomical origin and diagnostic relevance of the sub-types remain to be explored, although some ELONGATE ENTIRE with cylindrical cross section seem to be associated with fiber cells in, for example, grasses.

Some opal sponge spicules, known as megascleres, present an elongate outline and can be confusers with the cylindrical sub-type, especially if fragmented (Fig. 4N). However, if an axial canal can be observed, the morphotype can unambiguously be assigned as a sponge spicule rather than ELONGATE ENTIRE, which should never have this feature (for illustrations, see Boury-Esnault and Rutzler, 1997).

Synonyms: Rods with smooth outlines (Baker, 1960). Cylindroid, rod (Parry and Smithson, 1964; Rovner, 1983). Elongate smooth (Twiss *et al.*, 1969, 4a). Plate or sheet element (Brown, 1984; Kaplan *et al.*, 1992). Sheet element with entire margin (Kaplan *et al.*, 1992, 156, Fig 8.1). Stretched (Colliot *et al.*, 1997, p. 278). Dicot long (Cummings, 1998, p. 105). Dicot 3D long (Cummings, 1998, p. 106). Parallelepiped elongate psilate and Cylindroid psilate (Albert *et al.*, 1999). Category A1 and A3 (Runge, 1999, p. 31). Elongate-rectangular with smooth edges (G 4.1) (Runge, 1999, Table 2). Linear (Madella *et al.*, 2002). Rectangular plate with straight edges (Blinnikov *et al.*, 2002, Fig. 3.1). "Smooth elongate" (Elo-1), Thick, trapezoidal "smooth elongate" (Elo-2) (Strömberg, 2003, p. 315, Fig. 4.12a). Smooth cylindric rod (Elo-7) (Strömberg, 2003, p. 315, Fig. 4.12g). Plate-like bar (Lu and Liu, 2003). Sclereid (Piperno, 2006, p. 112, Figs. 6.1d-e, Garnier *et al.*, 2016, Fig. 2Ae). Subepidermal rod phytolith (Ball *et al.*, 2009). Cylindroid large (Mercader *et al.*, 2009, Fig. 2j). Tabular elongate (Mercader *et al.*, 2009, Fig. 4k). Tabular psilate (Mercader *et al.*, 2009, Fig. 2n). Tabular thick sinuate (Mercader *et al.*, 2009, Figs. 6d,e). Tabular scrobiculate (Mercader *et al.*, 2009, Fig. 2q, Mercader *et al.*, 2010, Fig. 5.10). Tabular sinuate (Mercader *et al.*, 2010, Fig. 5.11). Tabular thin (Mercader *et al.* 2010, Fig. 5.12). Cylindroid (Mercader *et al.*, 2011, Fig. 2i). Tabular thick sinuate (Mercader *et al.*, 2011, Fig. 2o). Elongate smooth (Gu *et al.*, 2013,

Fig. 2D). Elongate tenius lacunose (Phillips and Lancelotti, 2014, Fig. 3ac). Rectangular elongate blocky (Phillips and Lancelotti, 2014, Fig. 3ae). Cylindroid with ridge (Phillips and Lancelotti, 2014, Fig. 3aa). Cylindric geniculate psilate (Garnier *et al.*, 2016). Non-diagnostic elongate (Bremond *et al.* 2016, Fig. 2l). Elongate psilate (Calegari *et al.*, 2017, Fig. 4b; Gomes Coe *et al.*, 2017, Fig. 8G). Elongate, Elongate entire, Elongate entire granulate, Elongate entire psilate, Elongate entire rugose, Elongate thick (PhytCore: www.phytcore.org).

Illustrations: Fig. 4A-M.

ELONGATE SINUATE

Code: ELO_SIN

Rationale for naming: ELONGATE SINUATE is produced by several groups of modern land plants; thus, a taxonomic name is not appropriate. Because their anatomical origin is also not always known, it is necessary to give them a morphological name. It is characterized by its elongate shape and sinuate margins.

Description: Tabular, with an overall rectilinear to nearly rectilinear 2D outline. L:W is ≥2. The margins of the long sides (rarely the short sides) are distinctly sinuate, with alternating convexities and concavities. The amplitude and periodicity of the undulating concavities and convexities are variable and can be regular or irregular. Undulations can range from slightly too well developed, in the latter case sometimes becoming clavate to columnar to castellate. Surface texture can vary widely including psilate, granulate, papillar, and striate. Often observed as single cells, but also occurring articulated.

Size: Length 50-200 µm.

Anatomical origin and taxonomic occurrence: ELONGATE SINUATE seem to be restricted to the leaf epidermis in plants of various taxonomic affiliations. In grass leaves, they are formed in the long cells (Metcalfe, 1960; Barthlott and Martens, 1979; Gallego and Distel, 2004). A special type not observed outside of Poaceae is an ELONGATE SINUATE with very distinct concave ends which result from partial encompassing of stomata or short cells (e.g. Metcalfe, 1960, Figs. 10-11; Gallego and Distel, 2004, Fig. 3D). ELONGATE SINUATE have also been observed in the leaf epidermis of Cyperaceae (Metcalfe, 1971, 15, Fig. 5; Fernandez Honaine *et al.*, 2009), Marantaceae (Fig. 4O), Pinaceae (Klein and Geis, 1978, Fig. 9; Sangster *et al.* 1997; Strömberg, 2003), and Polypodiopsida ("ferns" including horsetails; Strömberg, 2003; Mazumdar, 2011, Fig. 1c).

Discussion and interpretation: ELONGATE SINUATE varies in how sinuate the margins are. Sometimes only one of the long sides is sinuate, while the other one is entire (Fig. 4R). Transitional forms with ELONGATE ENTIRE, ELONGATE DENTATE and ELONGATE DENDRITIC occur. In the leaf epidermis of Poaceae and other monocotyledons, numerous ELONGATE SINUATE form silica skeletons which can be preserved in soils, sediments and archaeological sites. They may, however, only be attributed to Poaceae in the presence of other typical morphotypes, such as short cells, trichomes (ACUTE BULBOSUS), PAPILLATE and stomata of the graminaceous type (Metcalfe, 1960).

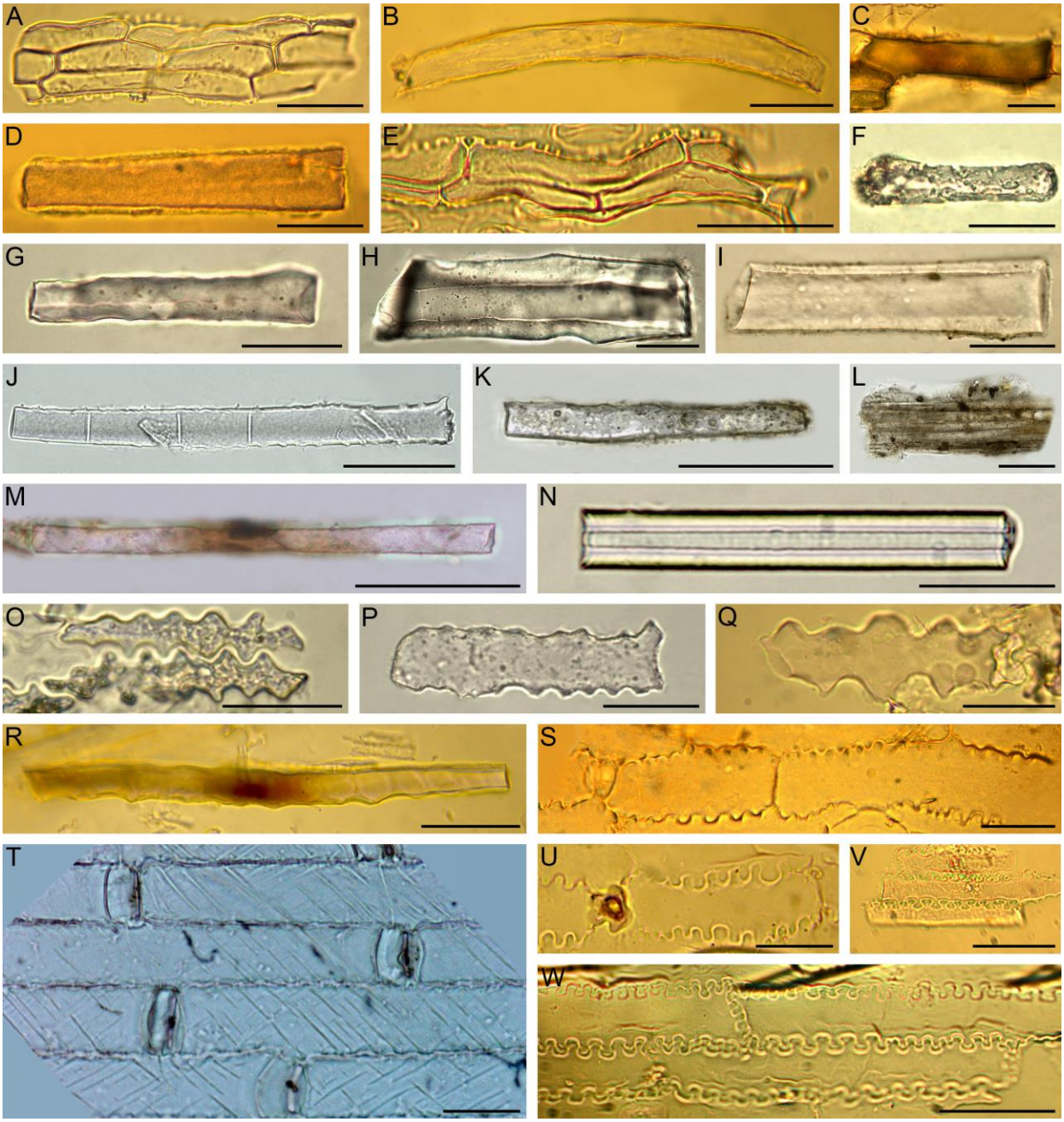

FIG. 4. (A-M) ELONGATE ENTIRE and transitional forms, single and articulated, (A) *Loudetia togoensis* (Poaceae), leaf (PHV 15), (B) *Brachiaria jubata* (Poaceae), leaf (PHV 259), (C) *Panicum subalbidum* (Poaceae), leaf (PHV 249), (D) *Andropogon gayanus* (Poaceae), leaf (PHV 256), (E) *Loudetia togoensis* (Poaceae), leaf (PHV 296), (F-I) Archaeological samples, Mali and Cameroon, (J) *Macaranga heudelotii* (Euphorbiaceae), bark (PHV 797), (K-M) Archaeological soil thin sections, Brussels (Belgium), (N) Potential confuser: Sponge spicule fragment, soil sample, Cameroon, (O-W) ELONGATE SINUATE and transitional forms, single and articulated, (O) *Sarcophrynium brachystachyum* (Marantaceae), leaf (PHV 89), (P) Archaeological sample, Cameroon, (Q) *Sorghum aethiopicum* (Poaceae), leaf (PHV 242), (R) *Pennisetum pedicellatum* (Poaceae), leaf (PHV 251), (S) *Panicum turgidum* (Poaceae), leaf (PHV 250), (T) *Triticum aestivum* (Poaceae), stem, (U) *Hackelochloa granularis* (Poaceae), leaf (PHV 263), (V) *Cymbopogon giganteus* (Poaceae), leaf (PHV 266a), (W) *Heteropogon melanocarpus* (Poaceae), leaf (PHV

298). Scale A-I, N-Q, S-W: 20 µm; J-M, R: 50 µm. Authors: A-J, N-S, U-W: K. Neumann; K-M, T: E. Buchanan and M.J. Hodson. .

Synonyms: Elongate thin sinuous (1A1) (Brown, 1984, Fig. 1, 1A1a & c). Sheet element, margin sinuous (Kaplan *et al.*, 1992, p. 157, type Ia; Figs. 8.2 A, B). Sheet element, margin undulate-interlocking (Kaplan *et al.*, 1992, p. 157, type Ie: Figs. 8.3 A, B). Quadrilateral with undulating short edges, highly serrated edges, serrations rounded (Pearsall and Dinan, 1992, p. 57, Fig. 3.7A).. Wavy edged long cells (Sangster *et al.*, 1997). Wavy elongate (Epi-8) (Strömberg, 2003, Fig. 4.8a). Elongate-rectangular with sinuate or serrated edges (G 4.1) (Runge, 1999). Silica skeleton long cells wavy from grasses (Albert *et al.*, 2003, Fig. 5c). Tabular crenate (Mercader *et al.*, 2011, Fig. 2n). Leaf long sinuate (Weisskopf *et al.*, 2014, Fig. 2A). Long cell with protuberances (Madella *et al*., 2016). Elongate columellate (Gomes Coe *et al.*, 2017, Fig 4d). Elongate crenate (Gomes Coe *et al.*, 2017, Figs. 6D, 8L). Elongate sinuate (PhytCore: www.phytcore.org).

Illustrations: Fig. 4O-W.

ELONGATE DENTATE

Code: ELO_DET

ICPN 1.0: Elongate echinate long cell

Rationale for naming: ELONGATE DENTATE is produced by several groups of modern land plants; thus, a taxonomic name is not appropriate. Because their anatomical origin is also not always known, it is necessary to give them a morphological name. “Dentate” is the appropriate descriptor for margin features (whereas “echinate” is a surface ornamentation descriptor).

Description: Elongated, with a rectilinear to nearly rectilinear 2D outline. L:W is ≥2. The margins of the long side (rarely, if ever on the short side) in 2D view are dentate, i.e. they have acute, sometimes carinate projections. Their thickness can range from thinly tabular to robustly thick. Surface texture is typically psilate, but sometimes granulate, or papillar. Often observed as single cells, but also occurring articulated.

Size: Length 20-250 µm.

Anatomical origin and taxonomic occurrence: ELONGATE DENTATE are commonly formed in long cells in the epidermis of Poaceae leaves, connected with each other and with other epidermal elements (Fig. 5C). ELONGATE DENTATE have also been observed in other plant families, e.g., Marantaceae (Fig. 5M). This morphotype is common in the inflorescence of Poaceae where they form a continuum with ELONGATE DENDRITIC. In these cases, the lumina of long cells are infilled with silica, with the dentate margins being formed by the silicifying of plasmodesmata connecting adjacent cells.

Discussion and interpretation: Transitional forms with ELONGATE ENTIRE, ELONGATE SINUATE and ELONGATE DENDRITIC occur.

Sponge spicules with an echinate surface, especially when fragmented, are potential confusers with ELONGATE DENTATE (Fig. 5S, T). Spicules can, however, be recognized by their distinct axial canal, their cylindrical shape, and their regularly distributed spines which cover the complete surface, in contrast to ELONGATE DENTATE, whose acute projections are restricted to the margins of the cells.

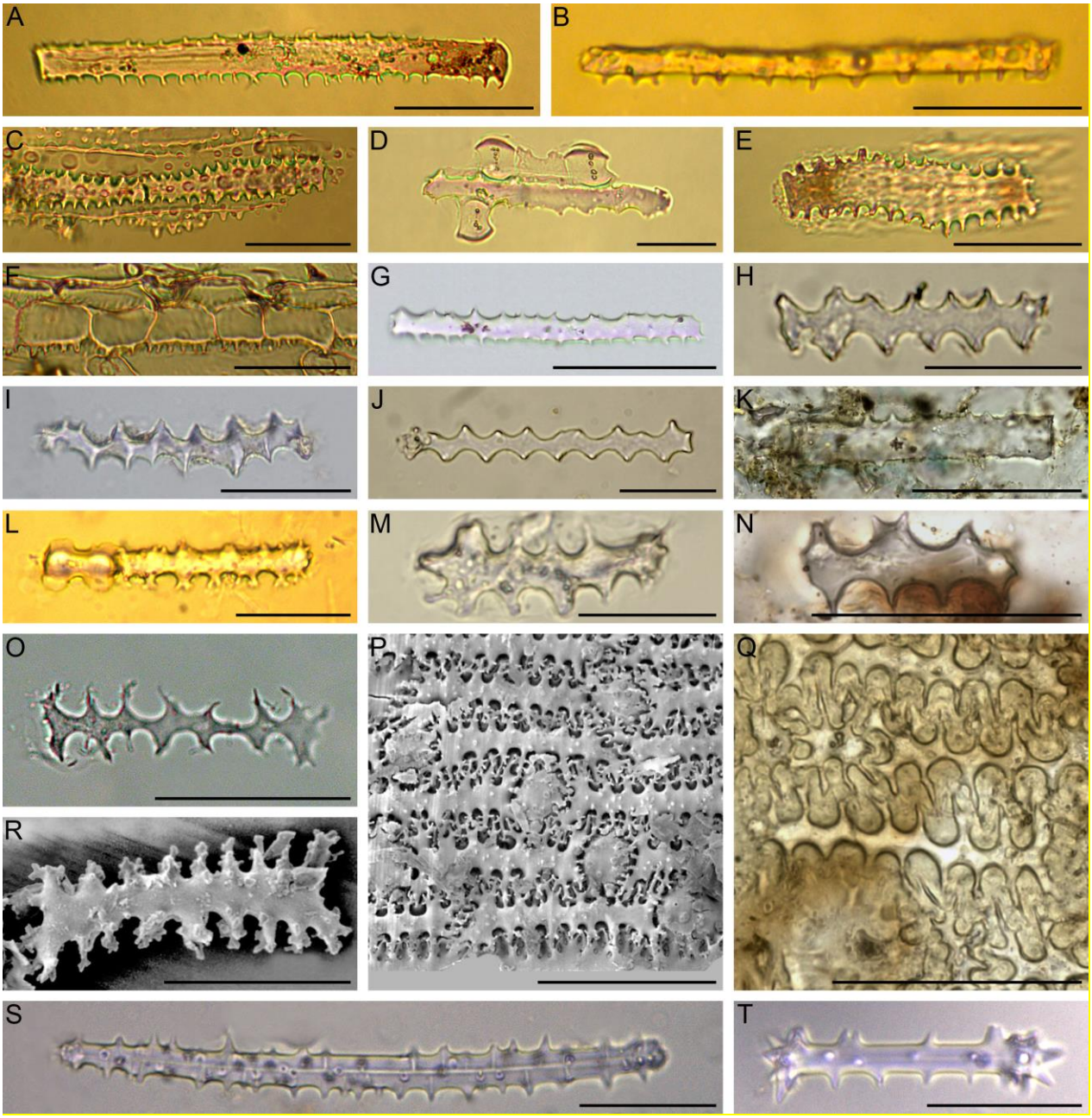

FIG. 5. (A-K) ELONGATE DENTATE, (A) *Loudetia togoensis* (Poaceae), leaf (PHV 296), (B) *Brachiaria lata* (Poaceae), leaf (PHV 260), (C) *Oryza barthii* (Poaceae), leaf (PHV 293), (D) *Schoenfeldia gracilis* (Poaceae), leaf (PHV 286), (E) *Oryza glaberrima* (Poaceae), leaf (PHV 289), (F) *Sorghum arundinaceum* (Poaceae), leaf (PHV 283), (G) *Aegilops speltoides* (Poaceae), inflorescence bract (RC_40), (H-J) Archaeological samples, Cameroon, (K) Archaeological soil thin section, Brussels (Belgium), (L-O) ELONGATE DENDRITIC, single cells, (L) *Panicum turgidum* (Poaceae), leaf (PHV 250), (M) *Sarcophrynium priogonium* (Marantaceae), leaf (PHV 179), (N) Archaeological soil thin section, Brussels, (O) *Triticum monococcum* (Poaceae), inflorescence bract, (P, Q) Articulated ELONGATE DENDRITIC, (P) *Triticum monococcum* (Poaceae), inflorescence bract (SEM), (Q) Archaeological soil thin section, Brussels, (R) ELONGATE DENDRITIC, single cell, *Triticum monococcum* (Poaceae), inflorescence bract (SEM), (S, T) Potential confusers: Sponge spicules, archaeological samples, DR Congo. Scale A-F, L: 20 µm; G-K, M-T:

50 µm. Authors: A-F, H-J, L, M: K. Neumann; G: R.M. Albert; K, N, Q: L. Vrydaghs; O, P, R: T. Ball; S, T: B. Eichhorn.

Synonyms: Elongate spiny with pavement (Twiss *et al.*, 1969, Fig. 2.4c, d). Intercellular silica (Geis, 1978, Plate 5F-H). Plate elongate thick (rounded top with pointed or rounded edges projections (Brown 1984, Fig. 1, IA2a). Long cell deeply indented (Blinnikov *et al.*, 2002, Fig. 3.6). Sinuate elongate (Lu and Kib, 2003, Plate 1, Fig. B). Elongate [Kondo *et al.* 1994, Plate 37b; Thorn 2004, Plates *Deschampia antartica* (p. 55) and *Dracophyllum scoparium* (p. 60)]. Spiny elongate (Epi-9) (Strömberg, 2003, Fig. 4.8b). Elongate spiny (Gallego and Distel, 2004, Fig. 3C; Fernandez Honaine *et al.*, 2006, Fig. 4d; Chauhan *et al.*, 2011, Fig 4H). Rod long smooth fibe wavy (Carnelli *et al.* 2004, Plate 2, Fig. 8). Elongate echinate (Bremond *et al.*, 2008, Fig. 2.9; Gu *et al.*, 2013, Fig. 2C; García-Granero *et al.*, 2016, Fig. 4a). Tabular lanceolate (Mercader *et al.*, 2009, Fig. 4O). Tabular dendriform (Mercader *et al.*, 2010, Fig. 5.7). Tabular/parallelepipedal bodies with echinate margin (Novello *et al.*, 2012, Plate II, El-3). Long epidermal cells with sinuate walls (Morcote-Rios *et al.*, 2015); l3e (Novello and Barboni, 2015, Plate 1B). Elongate cells with echinate walls (Jattisha and Sabu, 2012, Fig. 1, 4g). Elongate echinate long cell (Naskar and Bera, 2018, Plate 7, Fig. 3a-3c, 16a-16b). Elongate dentate (PhytCore: www.phytcore.org).

Illustrations: Fig. 5A-K.

ELONGATE DENDRITIC

Code: ELO_DEN

ICPN 1.0: Dendritic; Dentritic

Rational for naming: ELONGATE DENDRITIC is widely produced among modern land plants; thus, a taxonomic name is not appropriate. Because their anatomical origin is also not always known, it is necessary to give them a morphological name. The descriptor elongate is most appropriate for the first part of the name, referring to the general shape of the morphotype. The term dendritic as second part of the name refers to its characteristic margins.

Description: Elongate, with a rectilinear to nearly rectilinear 2D outline. L:W is ≥2. ELONGATE DENDRITIC typically have branched processes extending laterally away from both of their longer sides. Processes may also be observed extending laterally from the shorter ends of the phytolith. Though typically branched, the processes may range from branched once or multiple times to unbranched (i.e., dentate) on a single phytolith. The apices of the processes range from rounded to acute or dentate. Surface texture psilate to papillar.

Size: Length 20-250 µm.

Anatomical origin and taxonomic occurrence: ELONGATE DENDRITIC are most commonly formed in the long cells of the epidermis of the inflorescence bracts (palea, lemma and glume) of wild and domestic species of grasses. In the case of grasses, the dendritic processes appear to be formed by the silicifying of plasmodesmata connecting adjacent cells. The final shape and amount of branching of the processes might be correlated with the degree and timing of silicification.

ELONGATE DENDRITIC are abundantly produced in the tribes Triticeae and Aveneae, and other members of subfamily Pooideae, but have been reported in a wide range of other grass subfamilies (e.g., Pharoideae, Bambusoideae, PACMAD) as well (Parry and Smithson, 1966; Strömberg, 2003;

Novello and Barboni, 2015). In the Poaceae inflorescence bracts, they form a continuum with ELONGATE DENTATE. More rarely they occur in leaves of grasses (Fig. 5L) and other monocotyledons, such as sedges, palms, and Marantaceae (Fig. 5M), as well as in certain dicotyledons (e.g., Strömberg, 2003).

Discussion and interpretation: Transitional forms with ELONGATE ENTIRE, ELONGATE SINUATE and ELONGATE DENTATE occur.

Within archaeological and geologic deposits, ELONGATE DENDRITIC are frequently broken, but can also be found articulated in silica skeletons (Helbaek, 1960; Rosen, 1992; Berlin *et al.*, 2003; Petö *et al.*, 2013). Under light microscopy articulated ELONGATE DENDRITIC form wave lobes patterns corresponding to process shapes and their adjacent intercellular space. These wave patterns may be diagnostic at some taxonomic levels (Rosen, 1992; Ball *et al.*, 2016; Wang *et al.*, 2016).

ELONGATE DENDRITIC have been used to indicate domesticated cereals (Ishida *et al.*, 2003; Albert *et al.*, 2008; Devos *et al.*, 2009; Madella *et al.*, 2014; Portillo *et al.*, 2012; Power *et al.*, 2014; Rosen, 2010; Shillito, 2011; Zhang *et al.*, 2013), but are also common in wild grasses (Novello and Barboni, 2015). ELONGATE DENDRITIC from archaeological sites should therefore not *a priori* be attributed to domesticated cereals, unless the samples originate from secure contexts such as vessels known to be used for cereal storage or cooking (Berlin *et al.*, 2003; Petö *et al.*, 2013; Wang *et al.*, 2013) or in some cases, thin sections (Devos *et al.* 2013; Vrydaghs *et al.* 2016). Future systematic comparative studies of domesticated and wild taxa that produce ELONGATE DENDRITIC may help improve the taxonomic resolution of the morphotype. Ball *et al.* (2017) present preliminary data from a morphometric analysis of articulated ELONGATE DENDRITIC wave lobes. To date, their results show promise for archaeological applications, but also demonstrate intraspecific variation and the need for large comparative reference collections.

In their study of *Setaria italica* and *Panicum miliaceum*, Lu *et al.* (2009) name the Ω-undulated phytolith in *S. italica*, and η-undulated ones in *P. miliaceum* as "dendriform epidermal long cell." While the anatomical position in which they form is similar to that of the ELONGATE DENDRITIC, both undulating morphotypes have distinct morphological differences that separate them from ELONGATE DENDRITIC, the margins in 2D view being simple to complex clavate in case of the Ω shaped and simple to complex sinuate in case of the η-shaped undulations.

Synonyms: Dendriform (opals) (Parry and Smithson, 1966). Surface with protuberances branched dendritically (Ii) (Kaplan *et al.*, 1992, Fig. 8.4). Sinuous-walled long cells (Hodson and Sangster, 1988, Figs. 29, 30, 34, 43). Dendriform phytolith (Hodson and Sangster, 1988, Figs. 29, 30, 34, 43; Ball *et al.*, 1999, Figs. 8, 9). Elongate with branched processes (Epi-10) (Strömberg, 2003, Fig. 4.8c). Dendritics (El3d) (Novello and Barboni, 2015, Plate I). Non-diagnostic elongate (Bremond *et al.*, 2017, Fig. 2l). Dendritic long cells (Dal Corso *et al.*, 2017, Fig. 3g). Dendritic polylobate (Meister *et al.*, 2017, Fig. 7c). Elongate dendritic (PhytCore: www.phytcore.org)

Illustrations: Fig. 5L-R.

TRACHEARY

Code: TRA

Three subtypes: TRACHEARY ANNULATE/HELICAL (TRA_ANN), TRACHEARY PITTED (TRA_PIT), TRACHEARY BORDERED (TRA_BOR)

ICPN 1.0: Cylindric sulcate tracheid

Rationale for naming: Because the anatomical origin is clear and beyond doubt, an anatomical name can be given. This applies also for the terms pitted (Esau, 1965, 231) and bordered (Esau, 1965: 40).

Description: Shape varies from being more or less cylindric and elongate to more compact and polyhedral. Cylindric elongate bodies range from being relatively straight, with consistent diameter and unbranched to being any or all of irregular, ellipsoidal, brachiform, and having soft facets. Ends can be straight, rounded, or pointed/tapering. Phytoliths can consist of one or multiple of these bodies in articulation.

The characteristic feature of the morphotype is the surface decoration. In TRACHEARY ANNULATE/HELICAL this consists of ring- to helical-shaped ridges arranged perpendicular to the long axis, more or less regularly and densely distributed over the entire phytolith and appearing in side view as castellate protrusions at the long edges. In TRACHEARY PITTED, surface decoration consists of circular to oval projections in surface view, more or less densely distributed on the surface. In closer 3D-view these projections can show some variation, e.g. pilate, gibbate, or tuberculate, but never dendritic. They can be regularly arranged in vertical rows along the length of the phytolith or be less regularly arranged. In TRACHEARY BORDERED, surface decoration is characterized by small (~2-4 µm), convex discs with a centrally located, nipple-like knob that are commonly found in pairs on either side of the surface of the body as a whole, sometimes in addition to annulate/helical ridges.

Included in TRACHEARY are also transitional forms, for example morphotypes in which the ridges do not encircle the cylinder, but appear as narrow ellipses or oblong shapes on the surface of the body (oriented perpendicular to the long axis), as well as forms that are both annulate/helical and pilate. If a subtype cannot be clearly identified, the more general name TRACHEARY should be given.

The silicification of the TRACHEARY as a whole ranges from a thin interior layer with a hollow center to a completely infilled body.

Size: Length 15-200 µm, width 5-40 µm (varies greatly).

Anatomical origin and taxonomic occurrence: TRACHEARY phytoliths are interior casts of tracheary elements (tracheids or vessel elements) with ring or helical (spiral) thickenings on their inner cell wall surface (TRACHEARY ANNULATE/HELICAL), or with bordered pits in their cell walls (TRACHEARY PITTED, TRACHEARY BORDERED). In TRACHEARY ANNULATE/HELICAL, the sulcate (= furrowed) indentations between the ridges on the surface correspond to the former lignin-reinforced thickenings in the cell walls, whereas the ridges corresponds to the space between these thickenings which has been filled with silica. In TRACHEARY PITTED and TRACHEARY BORDERED, the projections correspond to the (partial to complete) silica infilling of bordered pits. The nipple-like knob in the center of the bordered pits in TRACHEARY BORDERED signifies the thickened torus of the pit membrane.

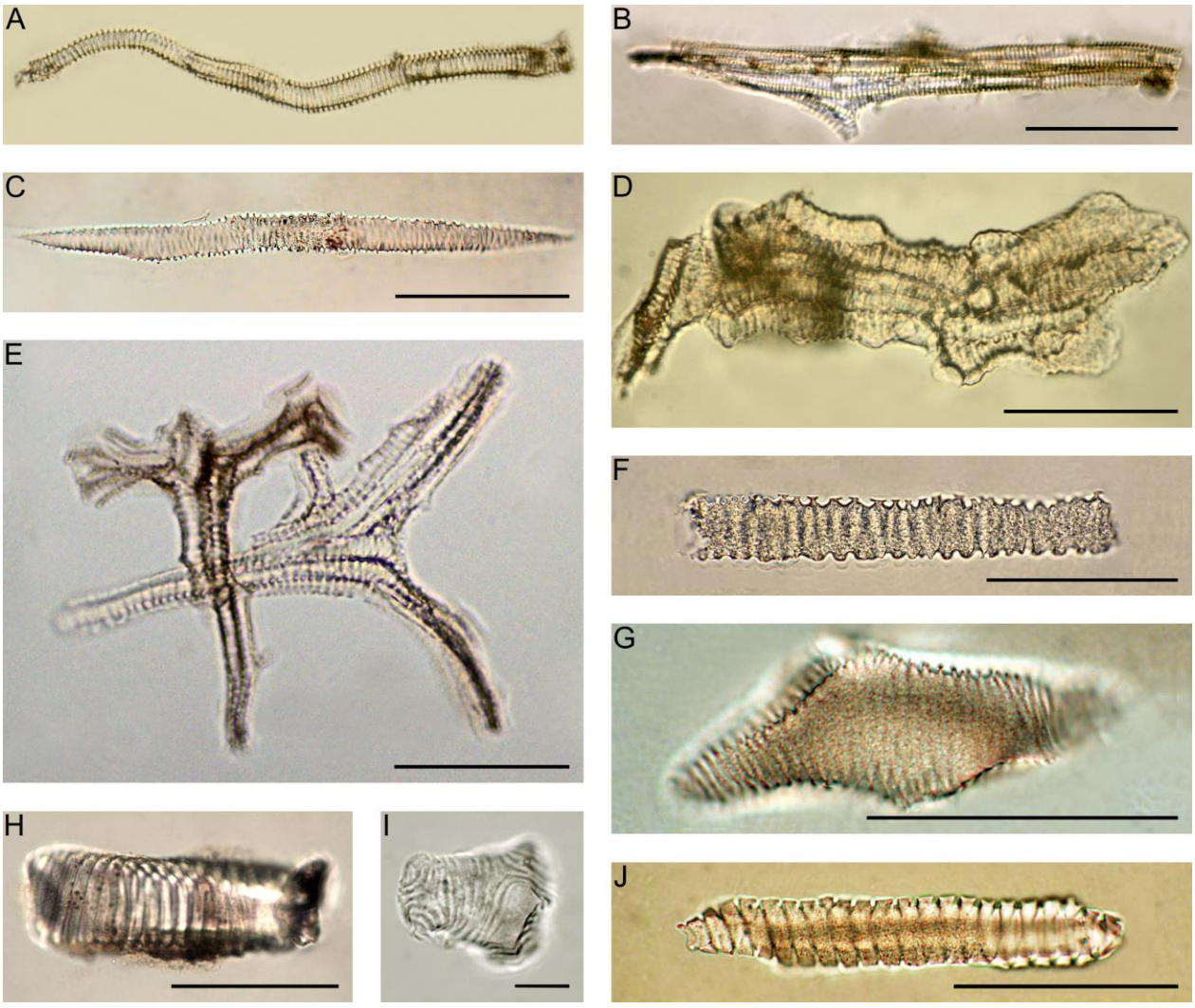

FIG. 6. TRACHEARY ANNULATE/HELICAL. (A) *Hypsodelphis violacea* (Marantaceae), leaf (PHV 466), (B) *Marantochloa filipes* (Marantaceae), leaf (PHV 467), (C) *Dryopteris* sp. (Dryopteridaceae), leaf (UCMP 399042), (D) *Annickia chlorantha* (Marantaceae), leaf (PHV 488), (E) *Populus nigra* (Salicaceae) (UBRC_VAL15_7_19), leaf, (F) *Larix* sp. (Pinaceae), leaf (UCMP 399064), (G) *Liquidambar* sp. (Altingiaceae), leaf (UCMP 399203), (H) *Selaginella* sp. (Selaginellaceae), leaf (UCMP 399040), (I, J) Soil surface samples from West Africa. Scale bar 100 µm. Authors: A, B, D, I, J: K. Neumann; C, F-H: C.A.E. Strömberg; E: R.M. Albert.

Although tracheids and vessel elements make up both primary and secondary xylem, they are mainly silicified in primary xylem. Thus, TRACHEARY phytoliths typically derive from leaves and herbaceous stems and roots (a rare possible exception has been observed in a secondarily thickened shoot of *Chimonanthus*; see Strömberg, 2003). They have also been observed in angiosperm fruits.

TRACHEARY is herein very broadly defined and includes tracheids and vessels. Tracheids are found in all groups of vascular plants, whereas vessels (consisting of vessel elements) are specialized tracheary elements found in most angiosperms, Gnetales, and some ophioglossoid ferns (Esau, 1965; Carlquist, 1996; Schneider and Carlquist, 1999). The end walls in tracheids are imperforated while in vessel elements they have perforations or are completely open (simple perforation). Silicified tracheids and vessel elements preserve evidence of the wall structure and the shape of their source cells (e.g. Raigemborn *et al.*, 2009); for this reason they can often be distinguished from each other. In addition, vessel elements can have more complex pitting and ribbing not observed in tracheids, thus allowing a closer taxonomic assignment of a phytolith.

TRACHEARY ANNULATE/HELICAL have a very wide taxonomic distribution, whereas the occurrence of TRACHEARY PITTED and TRACHEARY BORDERED seems to be more restricted. Long cylindric forms of TRACHEARY PITTED (Tra-8 by Strömberg, 2003), are commonly observed in Poaceae and some other monocots (e.g. palms). Shorter cylindroids and more irregular forms of TRACHEARY PITTED seem to occur in a limited number of arboreal taxa, including some gymnosperms (Kondo *et al.*, 1994; Wallis, 2003; Piperno, 2006: 37) and were first described by Postek (1981) from the leaves of *Magnolia* species. TRACHEARY BORDERED have so far only been observed in conifers and Gnetales (e.g. Klein and Geis, 1978; Strömberg, 2003; Thummel and Strömberg, unpublished data).

Discussion and diagnostic remark: TRACHEARY is produced by a wide range of plants; as such its diagnostic value is low. However, several authors have divided TRACHEARY more finely and used certain subtypes, for example the more irregular forms of TRACHEARY ANNULATE/HELICAL and TRACHEARY PITTED as indicative of non-grass plants, noting that grasses tend to produce mainly very straight TRACHEARY PITTED forms (e.g., Strömberg, 2004; Raigemborn *et al.*, 2009). Work is underway to provide a more finely subdivision of TRACHEARY (e.g., Strömberg, 2003).

The faceted terminal tracheids described from *Magnolia* leaves (Postek, 1981; Strömberg, 2003, Fig. 4.13j (Scl-3); Piperno, 2006) also show a ring- or helical-shaped decoration on the surface. This pattern may derive as an imprint from an adjacent tracheid/vessel or consist of silicification of both a sclereid and a tracheid/vessel. However, because they are characterized by their distinct facets, which are not typical of TRACHEARY ANNULATE/HELICAL, they are not included here.

TRACHEARY PITTED can be distinguished from sclereids, which also show numerous small projections on their surface. A closer look, preferably with SEM, reveals that the projections of silicified sclereids are not pilate, but baculate, corresponding to infillings of simple pits which are typical for sclerenchyma cells. The shape of sclereids is also usually more irregular. Vessels and tracheids in wood only very rarely silicify (Collura and Neumann, 2017). The silicified pitted 'vessels' and 'tracheids' often mentioned as specific for wood (e.g. Runge, 1999; Piperno, 2006, p. 42, Fig. 2.17e) are actually not; they must be attributed to primary plant organs (leaves and stems).

Synonyms: TRACHEARY ANNULATE/HELICAL: Silicified vascular cell (Geis, 1973, Figs. 49-51; Geis, 1978, Plate 5A). Single tracheary element (Geis 1978, Plate 5B). Xylem vessel (Geis, 1978, Plate 5C). Tracheary element (Klein and Geis 1978, Fig. 7). Blade shaped opals from xylem cells (Kondo and Peason, 1981, Fig. 5a-g). Silicified branched tracheary element with spiral thickenings (Bozarth, 1992, Fig. 10.3D). Tracheid phytolith (Kondo *et al.*, 1994, Plate 19c-f; Plate 22c, d). Type A2, rod with a ring- or spiral-shaped surface (Runge, 1999, Plate III2). Hollow helix (helical tracheary element) (Tra-1) (Strömberg, 2003, Fig. 4.8f). Worm/pupa-like, infilled helical tracheary

element (Tra-2) (Strömberg, 2003, Fig. 4.8g). Ornamented (conifer) 3D polyhedrons (Tra-5 Type B) (Strömberg, 2003, Fig. 4.9a). Branching element with fine striate perforations (tracheid) (Wallis, 2003, Fig. 21). Simple tracheid phytoliths (Piperno, 2006, Fig. 2.18d). Vessel member (Mercader *et al.*, 2009, Fig. 3a). Vessel laminate (Mercader *et al.*, 2010, Fig. 4.1). Vascular tissues (Gu *et al.*, 2013, Fig. 4D). Tracheary (Phytcore, www.phytcore.org).

TRACHEARY PITTED: Vessels (Scurfield *et al.*, 1974, Figs. 13-20). Phytolith of a tracheary element (Postek, 1981, Figs. 15, 16). Tracheid phytolith (Kondo *et al.*, 1994, Plate 20a-f). Large pitted rod (monocot-type) (Tra-8) (Strömberg, 2003, Fig. 4.9d). Ornamented (conifer) 3D polyhedrons (Tra-5 Type C) (Strömberg, 2003). Irregular body with verrucate nodes (Wallis 2003, Figs. 4, 5). Silicified tracheary elements (Piperno, 2006, Fig. 2.7).

TRACHEARY BORDERED: Conifer transfusion tracheary element? (Klein and Geis, 1978, Figs. 1, 5). Tracheids with bordered pits (Bozarth, 1993, Fig. 1c). Conifer transfusion tracheary element (Tra-4) (Strömberg 2003, Fig. 4.8i). Ornamented (conifer) 3D polyhedrons (Tra-5 Type A) (Strömberg, 2003, p. 663, Fig. 4.8j).

Illustrations: Figs. 6, 7.

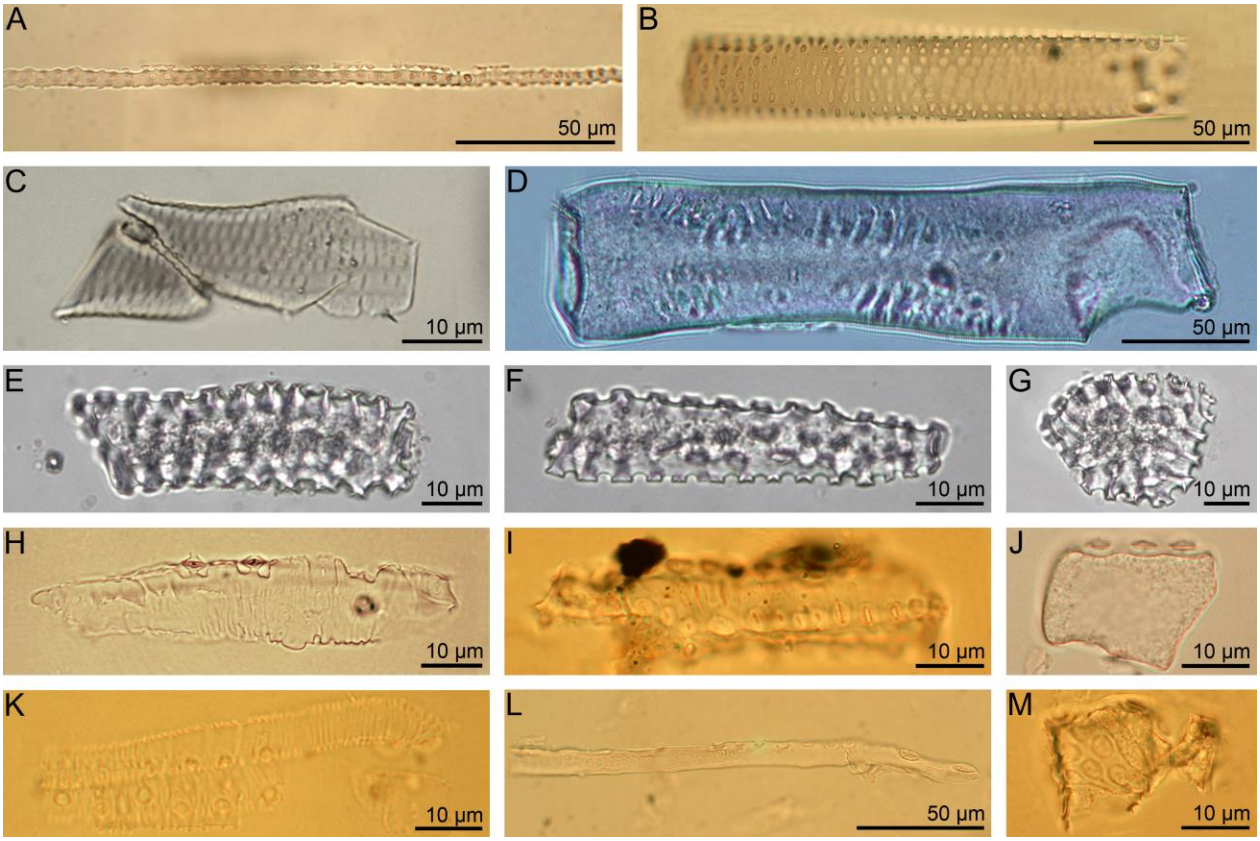

FIG. 7. (A-G) TRACHEARY PITTED, (H-M) TRACHEARY BORDERED. (A, B) *Otatea* sp. (Poaceae), culm, (C) Soil sample from archaeological site, Burkina Faso, (D) Soil surface sample, Costa Rica, (E-G) Soil surface sample, Burkina Faso, (H) *Abies* sp. (Pinaceae), leaf, (I) *Sequoia sempervirens* (Cupressaceae), leaf, (J, K) *Thuja occidentalis* (Cupressaceae), leaf, (L, M) *Podocarpus richei* (Podocarpaceae), leaf. Authors: A, B, H-M: C.A.E. Strömberg; C, E-G: K. Neumann; D: C. Crifò.

Grass silica short cell phytoliths (GSSCP)

General comments that apply to all GSSCP:

Grass silica short cell phytoliths form in specialized, silica accumulating short cells in the epidermis of members of the grass family (Poaceae).

Directional descriptors for GSSCP

Note: If at all possible, a description of GSSCP shape should include a description of the orientation in the grass epidermis under *"Orientation in epidermis,"* that is, whether its long axis (side) is parallel with the long axis of the leaf. Detailed information on the orientation of short cell phytoliths in the grass epidermis can be found in Watson and Dallwitz (1992 onwards), Rudall et al. (2014) and the atlasses on East African grasses (e.g., Palmer and Tucker, 1981, 1983; Palmer *et al*., 1985; Palmer and Gerbeth-Jones, 1986).

Outer periclinal surface/aspect (OPS): the GSSCP aspect facing outwards, towards the epidermal surface (for a discussion of GSSCP orientation in relation to the leaf surface, see Parry and Smithson, 1964, Text-Fig. 2). The OPS is usually larger than the inner periclinal surface (IPS, see below), often somewhat concave, and not ornamented (see also Mulholland, 1989; Mulholland and Rapp, 1992). Under light microscopy the OPS has clear distinct edges that are more well defined, crisp, and clear than those of the IPS. Previous authors have referred to the OPS as the base (e.g., Mulholland 1989; Mulholland and Rapp, 1992), bottom (e.g., Piperno, 1984), or thick face (e.g., Chávez and Thompson, 2006).

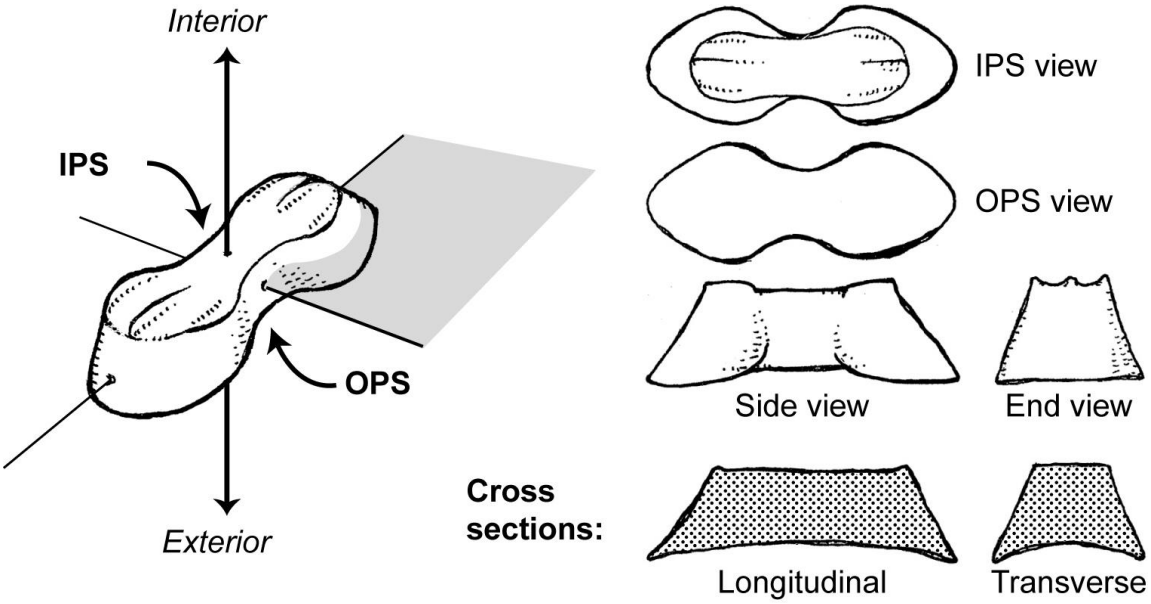

FIG. 10. Directional descriptors for GSSCP. IPS = inner periclinal surface/aspect; OPS = outer periclinal surface/aspect. Grey surface = parallel with epidermal surface. Adapted from Strömberg (2003).

Inner periclinal surface/aspect (IPS): the GSSCP aspect opposite the OPS, whether a keel, plateau, or a more complex surface, facing inwards, towards the interior of the plant tissue (for a discussion of GSSCP orientation in relation to the leaf surface, see Parry and Smithson, 1964: Text-Fig. 2). Under light microscopy the IPS is typically less well defined, crisp, and clear than the OPS. The IPS is often, but by no means always, smaller and can be highly ornamented, or faceted. Previous authors have referred to it as the top (e.g., Piperno, 1984; Mulholland 1989; Mulholland and Rapp, 1992; Fredlund and Tieszen, 1994), or thin face (e.g., Chávez and Thompson, 2006).

Side: the longest pair of four lateral faces connecting the IPS and the OPS of GSSCP, regardless of orientation in the leaf epidermis (see also Mulholland, 1989; Mulholland and Rapp, 1992).

Side view: view of the side of GSSCP.

End: the shortest pair of four lateral faces connecting the IPS and the OPS of GSSCP, regardless of orientation in the leaf epidermis (see also Mulholland, 1989; Mulholland and Rapp, 1992).

End view: view of end of GSSCP.

IPS view: Seen at right angle to the IPS/OPS of GSSCP, with the IPS proximal.

OPS view: Seen at right angle to the IPS/OPS of GSSCP, with the OPS proximal.

Planar view: IPS or OPS view of GSSCP (Pearsall, 1982; Mulholland, 1989; Mulholland and Rapp, 1992), referred to as abaxial/adaxial outline by Fredlund and Tieszen (1994).

Cross sections:

Longitudinal section: section of GSSCP along a plane parallel to side view.

Transverse section: section of GSSCP along a plane parallel to end view.

Other terms:

PACMAD: Clade of tropical grasses, including members of the Panicoideae, Arundinoideae, Chloridoideae, Micrairoideae, Aristidoideae and Danthonioideae subfamilies (Grass Phylogeny Working Group II, 2012; Soreng *et al*., 2015).

SADDLE

Code: SAD

ICPN 1.0: Saddle

Rationale for naming: SADDLE is considered a *nomen conservandum* from Fredlund and Tieszen (1994: Fig. 2G, H), who provided very clear, three-dimensional illustrations of this morphotype, the "classical" saddle.

Description: Symmetrical morphotype described as resembling a saddle (e.g., Metcalfe, 1960) or a battle axe with double edges (Prat, 1948), in planar view consisting of two more or less convex faces connected by concave faces. In side view, both IPS and OPS are concave; in end view, IPS and OPS are typically convex. In planar view, IPS and OPS have the same, or nearly the same, size and shape, giving the body nearly three planes of symmetry.

SADDLE encompasses morphotypes with the convex faces (slightly) shorter than, or equal to the concave faces, sometimes referred to as "tall" saddle, as well as forms with longer convex faces, so-called "squat" saddles (Piperno and Pearsall, 1998: Figs. 18-20).

Size: Typically 8-20 µm (longest axis).

Orientation in epidermis: In all SADDLE reported to date, the convex "battle axe edges" are parallel with the long axis of the leaf (Metcalfe, 1960; Rudall *et al.*, 2014).

Taxonomic occurrence: SADDLE have primarily been described from grasses in the Chloridoideae subfamily (e.g., Twiss *et al.*, 1969; Fredlund and Tieszen, 1994), but, in particular the "tall" form is also occasionally produced in several taxa within early-diverging grasses and the Bambusoideae, and in non-chloridoid C_3 and C_4 PACMAD grasses (Kondo *et al*., 1994; Strömberg, 2003) - although it should not be confused with so-called collapsed saddles (e.g., Piperno and Pearsall, 1998; Strömberg, 2003; Neumann *et al.*, 2017).

Discussion and interpretation: Morphotypes that are similar to SADDLE but where the IPS and OPS differ in shape or size in side/end or planar view (resulting in <3 planes of symmetry) are herein excluded from the "classical" SADDLE. These morphotypes, which include so-called collapsed saddles, plateaued saddles and saddles/bilobates (Piperno and Pearsall 1998), could instead be given a name with additional descriptors, such as SADDLE COLLAPSED (SAD_COL), or SADDLE PLATEAUED (SAD_PLA) etc. The "very tall saddle" morphotype with a length of the concave sides greater than 15 µ*m*, as described by Piperno and Pearsall (1998) and quantified in two species of Bambusoideae (Yost et al., 2018), differs from SADDLE in being longer, having deeply concave sides in planar view, and in that the shape of its OPS and IPS differs substantially in both planar view (i.e., whereas the IPS ends are convex, the OPS ends appear almost straight) and side view.

Because SADDLE is most commonly found in chloridoid grasses, it is frequently used as diagnostic of C_4 grasses in the Chloridoideae, and is as such meaningful in the calculation of the Iph index (e.g., Alexandre *et al.*, 1997; Barboni *et al.*, 2007). However, as "tall" saddles are found in other grass subfamilies, the taxonomic affiliation of SADDLE may in some cases be dependent on context (i.e., having *a priori* knowledge of local grass communities or rely on assessment of the combination of different GSSCP morphotypes).

Synonyms: Saddle-shaped (in part) (Metcalfe, 1960, Fig. I 9 (iv)-(viii)). Chloridoid Class (2a-b, in part) (Twiss *et al.*, 1969, Fig. 2). Doliolita (at least in part) (Bertoldi de Pomar, 1971, 323, "Clave gráfica"). Widely saddle-shaped (in part) (Palmer and Gerbeth-Jones, 1988, e.g., Fig. 97*d*). Saddle Narrow (in part, IVA2a) and Wide (in part, IVB2b) (Brown, 1984, Fig. 1). True saddle (SA-1) (Strömberg, 2003, Fig. 4.20f, g). Saddles with short/long convex edges, saddle symmetrical with concave and convex edges of the same length (Barboni and Bremond 2009, Fig. 1, 39-41). Saddle (PhytCore:www.phytcore.org).

Illustrations: Fig. 8Bb-Ff.

BILOBATE

Code: BIL

ICPN 1.0: Bilobate short cell

Rationale for naming: BILOBATE is here expanded from Brown's (1984: Fig. 1) morphotype class VI. Although Brown's (1984) definition of Bilobates, similarly to ours, includes a wide range of shapes and ornamentations, he did not discuss the "vertical" bilobates of Oryzoideae. Herein BILOBATE is defined as including all forms with two lobes, regardless of orientation.

Description: Morphotype whose OPS consists of two lobes separated by two indentations or a distinct castula, with length ≥1.3 the width of the lobes (planar view). OPS ends convex, straight, or concave (planar view). IPS variable in shape (bilobate, angular, to carinate in IPS view), size relative to OPS, and degree and type of ornamentation (e.g., ridges, tubercles). Thickness variable.

Size: Long axis typically 10-25 µm, occasionally up to 40 µm.

Orientation in epidermis: In most grasses, the long axis (side) of BILOBATE is parallel with the long axis of the leaf. However, in some grass taxa, notably the Oryzoideae, BILOBATE has its long axis perpendicular to the long axis of the leaf.

Taxonomic occurrence: BILOBATE (as broadly defined herein) have been described from nearly all subfamilies of grasses except the early-diverging Anomochlooideae (Watson and Dallwitz, 1992 onward; Prasad et al., 2005; Piperno, 2006; Rudall et al., 2014). In Pooideae, they have primarily been described from the tribe Stipeae, but can occur in other pooid taxa in low frequencies as well (e.g., Fredlund and Tieszen, 1994; Kerns, 2001; Strömberg, 2003; Blinnikov, 2005).

Discussion and interpretation: BILOBATE comprises a broad set of morphotypes that is often sub-divided to distinguish forms produced by different subclades (e.g., Piperno and Pearsall, 1998; Strömberg *et al.*, 2013). For example, *Oryza* and relatives make BILOBATE with distinctly "scooped" sides (Prasad *et al.*, 2011; Neumann *et al.*, 2017), whereas certain pooid grasses in the tribe Stipeae produce BILOBATE with poorly separated lobes and trapezoidal longitudinal sections (Fredlund and Tieszen, 1994).

BILOBATE can be distinguished from CROSS by having a long axis >1.3 the width of the lobes (planar view). This cutoff conforms closely to that used by Pearsall (1978) over the most common GSSCP size range (Radomski and Neumann, 2011). BILOBATE can be distinguished from POLYLOBATE by the absence of one or more clearly separated, additional lobes inserted between the two primary lobes.

Because BILOBATE can be found in taxa from across the Poaceae, its taxonomic use depends on *a priori* knowledge of local grass communities (e.g., Alexandre *et al.*, 1997; Barboni *et al.*, 1999, 2007), a more finely divided BILOBATE morphospace (e.g., Lu and Liu 2003; Strömberg, 2005; Fahmy 2008; Novello *et al.*, 2012; Neumann *et al.*, 2017), or both.

Synonyms: Dumb-bell shaped, *Oryza* type (Metcalfe, 1960, Figs. IA.17-18, IB.19-23). Panicoid Class: Dumbbell (3c-3f) (Twiss *et al.*, 1969, Fig. 2). Halteriolita variants 4-12 (Bertoldi de Pomar, 1971, "Clave gráfica," p.323). Bilobates (VI) (Brown, 1984, Fig. 1). Dumbbell (Mulholland, 1989, Fig. 2). *Stipa*-type, Simple Lobate, Panicoid-type (Fredlund and Tieszen, 1994, Fig. 2F-H). Bilobate (PhytCore:www.phytcore.org).

Illustrations: Fig. 8A-N.

POLYLOBATE

Code: POL

ICPN 1.0: Cylindrical polylobate

Rationale for naming: POLYLOBATE is considered a *nomen conservandum* from Mulholland (1989, p. 495), who described these forms as bilobates "with more than the two end lobes."

Description: Morphotype consisting of two end-lobes separated by a castula, along which are inserted additional, distinctly separated lobes (in effect a BILOBATE with additional lobes attached along an extended castula). Castula-lobes can be of similar size or smaller than end lobes and either paired (present on both sides of the castula) or unpaired. Both IPS and OPS are lobed in shape, although the IPS can be less well defined in castula areas. IPS can be ornamented (e.g., ridges, tubercles).

Size: Long axis typically 20-40 µm.

Orientation in epidermis: In POLYLOBATE reported to date, the long axis (side) is parallel with the long axis of the leaf.

Taxonomic occurrence: POLYLOBATE have been described primarily from the Panicoideae and other PACMAD grasses (e.g., Twiss *et al.*, 1969; Fahmy, 2008; Neumann *et al.*, 2017).

Discussion and interpretation: POLYLOBATE can be distinguished from BILOBATE by the presence of one or more clearly separated, additional lobes inserted between the two primary lobes (planar view).

POLYLOBATE can be distinguished from CRENATE in that it has an overall BILOBATE character due to well defined end lobes and castulae, but in addition has well defined lobes which are separately inserted (often resembling a string of pearls in IPS view) along the castula. CRENATE, on the other hand, have an overall rectangular shape in IPS view, with less well-defined castulae (Mulholland, 1989).

POLYLOBATE has mainly been used to indicate grasses in the Panicoideae and other (C_3/C_4) PACMAD taxa (e.g., Mulholland, 1989, Barboni *et al.*, 2007; Novello *et al.*, 2012).

Synonyms: Nodular (Metcalfe, 1960, Figs. IA 18 (i), IB 22 (iii)). Panicoid Class: Dumbbell spiny shank, Dumbbell nodular shank, Complex dumbbell (3g-j) (Twiss *et al.*, 1969, Fig. 2). Plurhalteriolita (in part) (Bertoldi de Pomar, 1971, 323, "Clave gráfica"). Polylobates (VII1a) (Brown, 1984, Fig. 1). Dumb-bell polylobate (Mulholland, 1989). Dumbbell complex (Mulholland and Rapp 1992, Fig. 4.16). Polylobate (PhytCore:www.phytcore.org).

Illustrations: Fig. 8W-Aa.

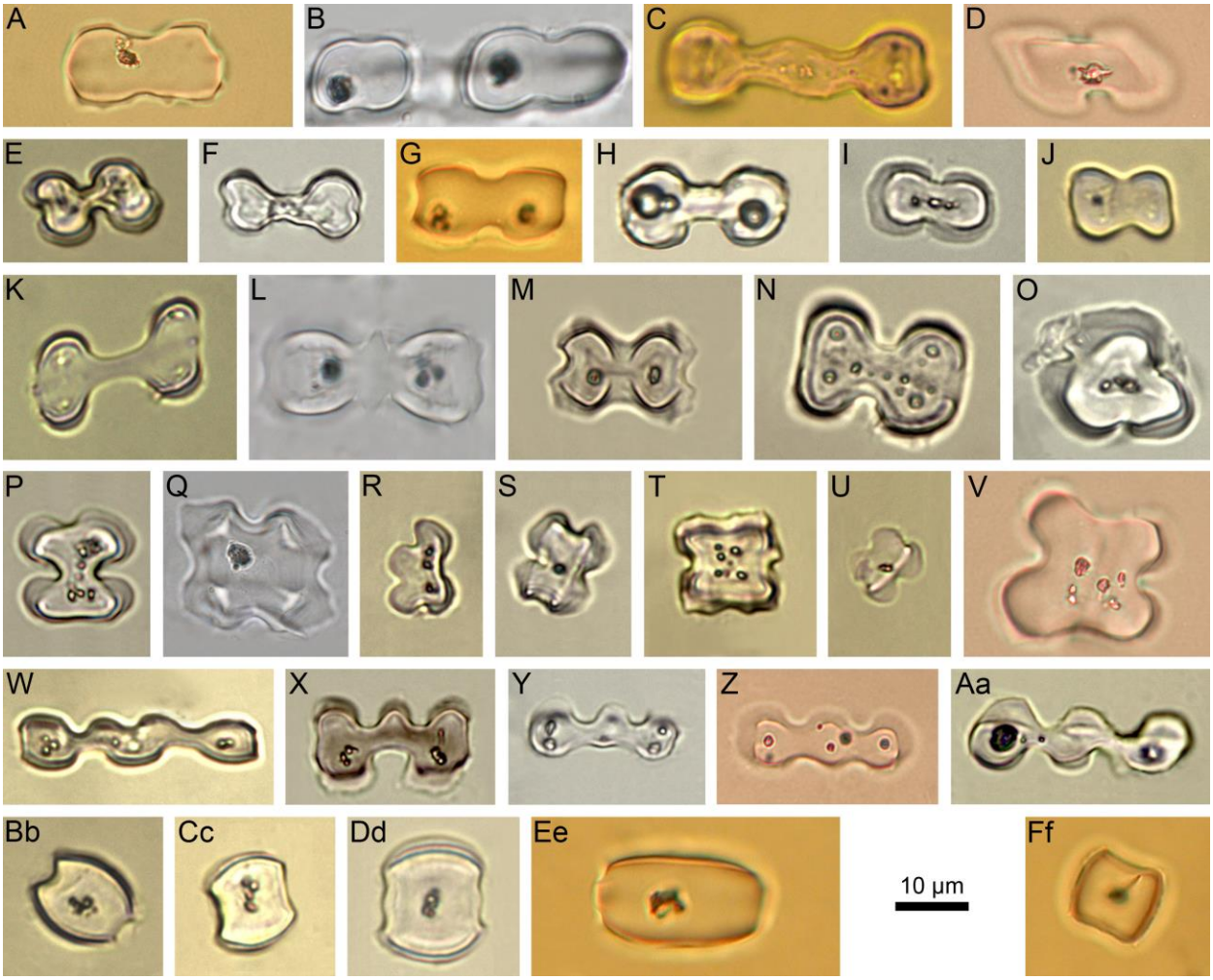

FIG. 8. BILOBATE, CROSS, POLYLOBATE, SADDLE, from Poaceae leaves, planar view. (A-N) BILOBATE. (A) *Nasella pulchra*, leaf (UCMP 399362), (B) *Chusquea longifolia* (UWBM PR 6204), (C) *Andropogon fastigiatus* (PHV 255), (D) *Glyceria striata* var. *striata* (UCMP 399356), (E) *Bracharia jubata* (PHV 304), (F) *Sorghum aethiopicum* (PHV 242), (G) *Eragrostis ferruginea* (UCMP 399353), (H) *Pennisetum polystachyon* (PHV 253), (I) *Andropogon gayanus* (PHV 256), (J) *Antephora nigritana* (PHV 275), (K) *Hyparrhenia involucrata* (PHV 299), (L) *Leersia ligularis* var. *grandiflora* (UWBM PR PR6191), (M) *Oryza longistaminata* (PHV 291), (N) *Hyparrhenia rufa* (PHV 246). (O-V) CROSS. (O) *Hyparrhenia involucrata* (PHV 299), (P) *Sorghum arundinaceum* (PHV 302), (Q) *Lithachne pauciflora*, (UWBM PR PR6667), (R) *Sorghum arundinaceum* (PHV 302), (S) *Brachiaria jubata* (PHV 304). (T) *Digitaria argillacea* (PHV 306), (U) *Vossia cuspidata* (PHV 277), (V) *Chasmanthium latifolium* (UCMP 399346). (W-Aa) POLYLOBATE. (W) *Pennisetum polystachyon* (PHV 253), (X) *Brachiaria lata* (PHV260), (Y) *Sorghum aethiopicum* (PHV 242), (Z) *Danthonia* sp. (UCMP 399350), (Aa) *Pennisetum pedicellatum* (PHV 303). (Bb-Ff) SADDLE. (Bb) *Tragus racemosus* (PHV 278), (Cc, Dd) *Schoenefeldia gracilis* (PHV 286), (Ee, Ff) *Eragrostis ferruginea* (UCMP 399353). Authors: A-B, D, G, L, Q, V, Z, Ee, Ff: C.A.E. Strömberg; C, E, F, H-K, M-P, R-U, W-Y, Aa-Dd: K. Neumann.

CROSS

Code: CRO

ICPN 1.0: Cross

Rationale for naming: CROSS is here expanded from the illustration in ICPN 1.0 (Madella *et al.*, 2005) to include all forms with three or more lobes separated by three or more (typically four) indentations in planar view.

Description: Morphotype whose OPS consists of three or more (typically four) roughly equal lobes separated by three or more (typically four) indentations. Length and width in planar view approximately equal, with longest dimension <1.3 times the length of the dimension at right angles with it. IPS variable in shape (e.g., cross, rectangular, rounded, carinate), size relative to OPS, and degree of ornamentation (e.g., facets, "flange"-like extensions, tubercles).

Size: Longest axis 8-35 µm.

Orientation in epidermis: In CROSS that are not perfectly equidimensional, the slightly longer axis (side) is parallel with the long axis of the leaf in most grasses. However, in some grass taxa, notably the Oryzoideae, CROSS have their long axis perpendicular to the long axis of the leaf.

Taxonomic occurrence: CROSS has been described from the Panicoideae and other PACMAD grasses, as well as from the Bambusoideae and Oryzoideae (Twiss *et al.*, 1969; Piperno and Pearsall, 1998; Strömberg, 2003; Prasad *et al.*, 2005, 2011; Fahmy, 2008; Barboni and Bremond, 2009; Novello *et al.*, 2012; Neumann *et al.*, 2017).

Discussion and interpretation: CROSS usually have four lobes, but three-lobed and five-lobed (etc.) forms are also included herein. The morphotype includes a wide range of forms that can be subdivided more finely to distinguish CROSS produced by different subclades (e.g., Piperno and Pearsall, 1998; Strömberg, 2003; Novello *et al.*, 2012; Neumann *et al.*, 2017). For example, *Chusquea* produces thick CROSS with a flat OPS and a larger IPS with irregular faceting, whereas many PACMAD grasses make relatively low CROSS with pronounced, rounded OPS lobes (e.g., Piperno and Pearsall, 1998; Strömberg, 2003; Prasad *et al.*, 2005, 2011).

CROSS can be distinguished from BILOBATE by having a long axis <1.3 the width of the lobes (planar view). This cutoff conforms closely to that used by Pearsall (1978) over the most common GSSCP size range (Radomski and Neumann, 2011).

CROSS are often used to estimate the abundance of grasses in the Panicoideae or even C_4 tall grasses within this clade in grassland ecosystems (e.g., Alexandre *et al.*, 1997; Piperno and Pearsall, 1998; Barboni *et al.*, 2007; Novello *et al.*, 2012; Neumann *et al.*, 2017); specific types are also used to infer the presence of Oryzoideae or Bambusoideae in the deep-time fossil record (e.g., Prasad *et al.*, 2005), or to track the domestication of *Zea mays* from archaeological deposits of the Neotropics (e.g., Pearsall, 1978; Piperno, 1983, 1984, 2009; Piperno *et al.*, 2009; Dickau *et al.*, 2012).

Synonyms: Cross-shaped (Metcalfe, 1960, Fig. IA 16). Panicoid Class: Cross (3a-b, in part) (Twiss *et al.*, 1969, Fig. 2). Euhalteriolita variant 14 (Bertoldi de Pomar, 1971, 323, "Clave gráfica,"). Crosses (VIII) (Brown, 1984, Fig. 1). Cross-shaped type (Pearsall, 1978). Cross (Mulholland, 1989; PhytCore:www.phytcore.org).

Illustrations: Fig. 8O-V.

CRENATE

Code: CRE

ICPN 1.0: Trapeziform polylobate, trapeziform sinuate

Rationale for naming: CRENATE is considered a *nomen conservandum* from Fredlund and Tieszen (1994: Fig. 2. E_1, E_2), who provided very clear, three-dimensional illustrations of this general morphotype. The term refers to the often crenate margins of the OPS.

Description: Morphotype characterized by, in planar view, overall rectangular shape but with sinuate to crenate OPS sides. Ends rectilinear, concave or (sometimes irregularly) convex. CRENATE typically has an asymmetrical trapezoidal cross-section, where the IPS usually is smaller than the OPS (but exceptions exist). IPS is overall rectangular but can have sinuate margins; it can also be ornamented (e.g., carinate or with small, marginal projections).

Size: Typically 20-60 µm long.

Orientation in epidermis: In CRENATE reported to date, the long axis (side) is parallel with the long axis of the leaf.

Taxonomic occurrence: CRENATE is found primarily in many members of the Pooideae subfamily but has also been recorded in low frequencies in certain early-diverging Poaceae lineages (*Pharus*, *Guaduella*) and PACMAD grasses (*Danthonia*) (e.g., Brown, 1984; Fredlund and Tieszen, 1994; Strömberg, 2003).

Discussion and interpretation: CRENATE can be separated from TRAPEZOID by the presence of clear undulations along the OPS (and sometimes also the IPS) margin.

CRENATE differs from POLYLOBATE in that the overall shape approximates a rectangle in planar view, whereas POLYLOBATE should evoke a BILOBATE with clear, additional lobes inserted between the end-lobes (i.e., the lobes are prominent and distinct enough that the overall shape is no longer rectangular). Some authors (Mulholland, 1989, Mulholland and Rapp, 1992) have devised a cutoff, whereby CRENATE should have a shaft/lobe ratio of >2/3 and POLYLOBATE <2/3, but we do not adopt this admittedly arbitrary guideline. Future work should attempt to establish a more quantitative and precise distinction between these morphotype classes that still reflects human perception of class membership (such as has been done for CROSS).

Because CRENATE is by far most commonly and abundantly produced by Pooideae, it is typically used as diagnostic of this grass subfamily, and often synonomous with cool temperate, C_3, and/or open-habitat grasses that today dominate at high latitudes or altitudes (e.g., Mulholland, 1989; Twiss, 1992; Fredlund and Tieszen, 1994; Barboni and Bremond, 2009).

Synonyms: Elongated-sinuous (Metcalfe, 1960, Figs. IA, 14-15). Festucoid Class: Oblong, sinuous (1h) (Twiss *et al.*, 1969, Fig. 2). (Lobed) costal and intercostal rods (Blackman, 1971, Figs. 104, 6-10, 13, 15, 19, 20). Plurhalteriolita (in part) (Bertoldi de Pomar, 1971, 323, "Clave gráfica"). Sinuous trapezoid (VA1 and VA2, in part) (Brown, 1984, Fig. 1). Sinuate polylobate (Mulholland and Rapp, 1992, Fig. 4.16). Pooid Class (1h) (Twiss, 1992, Fig. 6.1). Crenate (Fredlund and Tieszen, 1994, Fig. 2. E_1, E_2). Plate wavy, short, Plate wavy, long (Blinnikov, 2005, Plate 1,2-3). Long wavy plate (Morris, 2009, Plate II, g, n, p). Crenate (PhytCore:www.phytcore.org).

Illustrations: Fig. 9A-F.

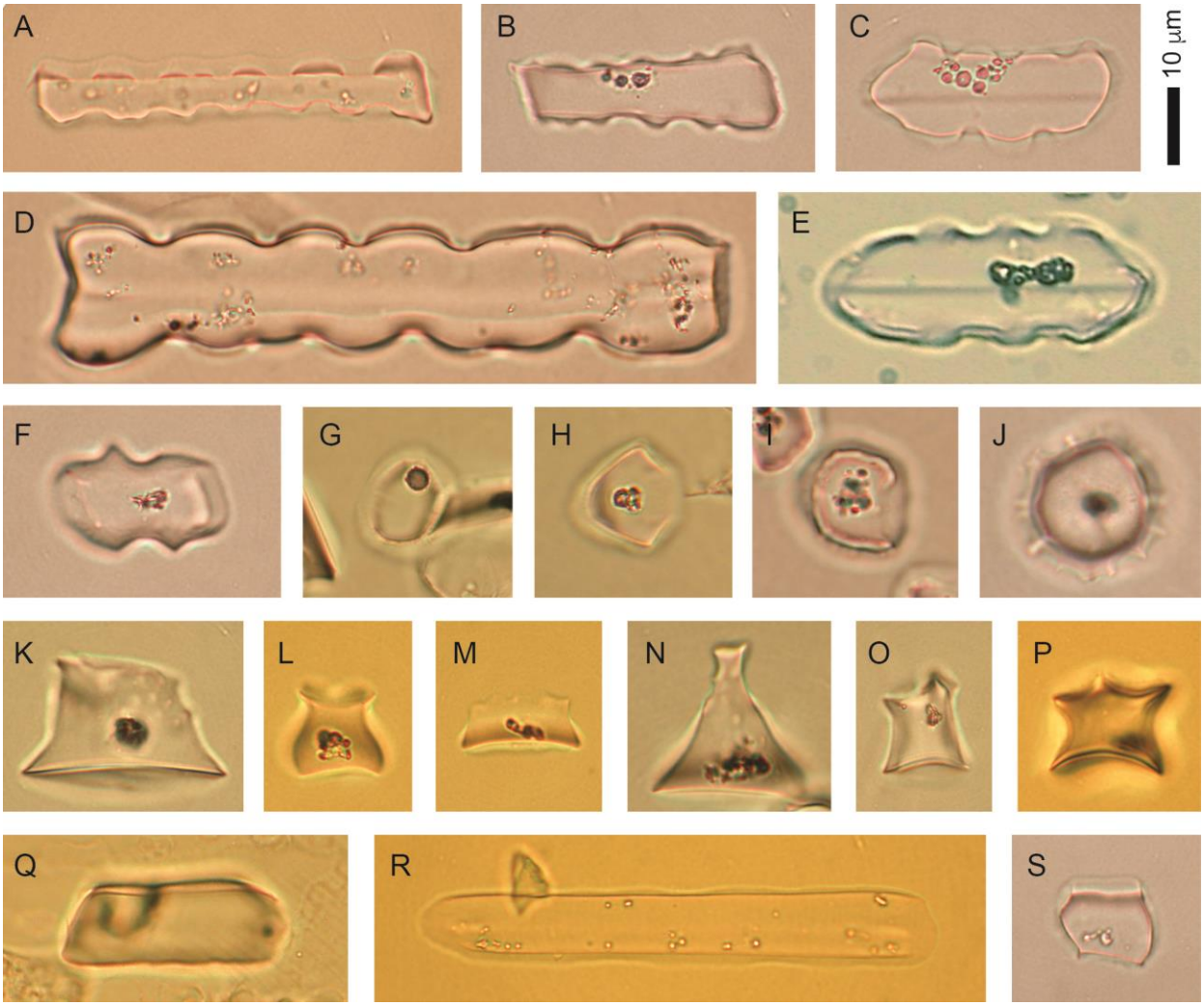

FIG. 9. CRENATE, RONDEL, TRAPEZOID from Poaceae. (A-F) CRENATE, planar view. (A, C) *Dactylis glomerata* ssp. *hispanica*, leaf (UCMP 399348), (B) *Lygeum spartum*, leaf (UCMP 399360), (D) *Avena fatua*, leaf (UCMP 399342), (E) *Triticum aestivum*, leaf (UBRC04_3_17), (F) *Calamagrostis ophiditis*, leaf (UCMP 399344). (G-P) RONDEL, (G-J) IPS view, (K-P) side view. (G, H) *Avena fatua*, spikelet (UCMP 399343), (I) *Sporobolus airoides*, leaf (UCMP 399372), (J) *Lygeum spartum*, leaf (UCMP 399360), (K) *Triticum aestivum*, leaf (UCMP 399374), (L) *Aristida purpurea* var. *wrightii*, leaf (UCMP 399340), (M) *Ampelodesmos mauritanicus*, leaf (UCMP 399338), (N) *Deschampsia caespitosa*, leaf (UCMP 399351), (O) *Chusquea patens*, leaf (UCMP 399347), (P) *Otatea acuminata* ssp. *aztecorum*, leaf (UCMP 399367). (Q-S) TRAPEZOID, planar view. (Q, R) *Festuca rubra*, leaf (UCMP 399354), (S) *Dactylis glomerata* ssp. *hispanica*, leaf (UCMP 399348). Authors: A-D, F-S: C.A.E. Strömberg; E: R.M. Albert**.**

RONDEL

Code: RON

ICPN 1.0: Rondel

Rationale for naming: RONDEL (after the Old French for "small circle") here conforms closely to Mulholland's (1989) definition, meaning that it is expanded from the illustration in ICPN 1.0 (Madella *et al.*, 2005) to include all forms with a roughly circular or oval OPS shape in planar view.

Description: Compact morphotype with approximately circular or oval OPS (planar view), which can be slightly indented or flattened along one aspect. IPS variable in shape (rounded to angular, pointed, or carinate), size relative to OPS (smaller, equal to, or larger), and degree and type of ornamentation (e.g., ridges, tubercles). RONDEL thickness also highly variable (low to very tall).

Size: OPS diameter generally 8-20 µm.

Orientation in epidermis: In RONDEL that are not perfectly equidimensional, the slightly longer axis (side) is often perpendicular to the long axis of the leaf.

Taxonomic occurrence: RONDEL have been described from nearly all subfamilies of grasses except the early-diverging Anomochlooideae (e.g., Piperno, 2006).

Discussion and interpretation: RONDEL herein encompasses a wide range of morphotypes that are commonly subdivided more finely, to distinguish RONDEL produced by different subclades (e.g., Piperno and Pearsall, 1998; Strömberg, 2003; Novello *et al.*, 2012). RONDEL can be separated from TRAPEZOID by their lack of parallel faces of the OPS in planar view.

Because certain types of RONDEL are often very abundant in members of the Pooideae, they have frequently been used as diagnostic of this clade (e.g., Twiss *et al.*, 1969; Fredlund and Tieszen, 1994; Barboni *et al.*, 1999, 2007; Blinnikov *et al.*, 2002). However, because of their wide occurrence in many Poaceae subfamilies (e.g., Mulholland, 1989; Novello and Barboni, 2015), the taxonomic use of RONDEL depends on *a priori* knowledge of local grass communities (e.g., Barboni and Bremond, 2009), a more finely divided RONDEL morphospace (e.g., Strömberg, 2005; Barboni and Bremond, 2009; Novello *et al.*, 2012; Neumann *et al.*, 2017), or both.

Synonyms: Round, Elliptical, Tall and narrow (Metcalfe, 1960, Figs. I 4,6-8). Festucoid Class: Circular, Elliptical, Acicular, Crescent (1a,c-e) (Twiss *et al.*, 1969, Fig. 2). Estrobilolita variants 19, 20, 22 (Bertoldi de Pomar (1971, 323, "Clave gráfica"). Double outline (IIIA2, IIIA3, in part), Trapezoids (VB2b1) (Brown, 1984, Fig. 1). Rondel (Mulholland, 1989). Conical, Keeled (Fredlund and Tieszen, 1994, Figs. A, B). Circular, waisted-cylindrical in side-view (G 1.5) (Runge 1999, Plate V, 9a). Conical rondels (CO, in part), Keeled rondels (KR, in part) (Strömberg, 2003, Figs. 4.19a-m). Rondel, Rondel tall (PhytCore:www.phytcore.org).

Illustrations: Fig. 9G-P.

TRAPEZOID

Code: TRZ

ICPN 1.0: Trapeziform short cell

Rationale for naming: Trapezoid is the shape that best describes the OPS shape of this morphotype in planar view (as well as its transverse and longitudinal sections).

Description: Both OPS and IPS quadratic to rectangular or oblong in planar view, with at least the two longer faces (sides) parallel, and with straight, convex, or oblique ends. IPS usually smaller, resulting in trapezoidal cross sections, and typically not strongly faceted or ornamented.

Size: Long axis 8-70 µm.

Orientation in epidermis: In TRAPEZOID reported so far, the long axis (side) is parallel with the long axis of the leaf.

Taxonomic occurrence: TRAPEZOID is produced by many Pooideae grasses. The morphotype has also been described from certain Bambusoideae (e.g., *Otatea*), early-diverging taxa (*Guaduella*, *Pharus*), and PACMAD grasses (e.g., *Aristida*, *Eragrostis*), in particular from reproductive organs (e.g., Brown, 1984; Mulholland, 1989; Strömberg, 2003).

Discussion and interpretation: RONDEL can be separated from TRAPEZOID by the shape of the OPS, which in RONDEL have no parallel faces in planar view.

TRAPEZOID can be separated from CRENATE by the absence of clear undulations along the OPS (and IPS) margin.

Long TRAPEZOID can be separated from ELONGATE ENTIRE by having several features typical of GSSCP, such as having a well-defined IPS and OPS, and a IPS that is often smaller, translucent material and well-defined 'pockets' of occluded carbon.

Because TRAPEZOID are often abundantly produced in many pooid grasses, they are frequently used as diagnostic of this clade (e.g., Twiss, 1992; Fredlund and Tieszen, 1994; Kondo *et al.*, 1994).

Synonyms: Elongated-smooth, Cubical, Cuboid (Metcalfe, 1960, Fig. IA 12). Festucoid Class: Rectangular, Oblong (1b,g, in part) (Twiss *et al.*, 1969, Fig. 2). Double outline (IIIA3, in part, III B1-4), Trapezoids: Non-sinuous (V, in part) (Brown, 1984, Fig. 1). Rectangle (Mulholland, 1989). Pyramidal (Fredlund and Tieszen, 1994, Fig. 2C).

Illustrations: Fig. 9Q-S.

LITERATURE CITED

Albert RM, Lavi O, Estroff L, Weiner S, Tsatskin A, Ronen A, LevYadun S. 1999. Mode of occupation of Tabun Cave, Mt Carmel, Israel during the Mousterian Period: A study of the sediments and phytoliths. *Journal of Archaeological Science* **26**: 1249-1260.

Albert RM. 2000. *Study of ash layers through phytolith analyses from the Middle Paleolithic levels of Kebara and Tabun cave (Israel).* PhD thesis. Universitat de Barcelona, Barcelona, Spain.

Albert RM, BarYosef O, Meignen L, Weiner S. 2003. Quantitative phytolith study of hearths from the Natufian and Middle Palaeolithic levels of Hayonim Cave (Galilee, Israel). *Journal of Archaeological Science* **30**: 461-480.

Albert RM, Shahack-Gross R, Cabanes D, Gilboa A, *et al.* 2008. Phytolith-rich layers from the Late Bronze and Iron Ages at Tel Dor (Israel): Mode of formation and archaeological significance. *Journal of Archaeological Science* **35**: 57-75.

Alexandre A, Meuniere JD, Lézine AM, Vincens A, Schwartz D. 1997. Phytoliths: indicators of grasslands dynamics during the late Holocene in intertropical Africa. *Palaeogeography, Palaeoclimatology, Palaeoecology* **136**: 213-229.

An X-H. 2016. Morphological characteristics of phytoliths from representative conifers in China. *Palaeoworld* **25**: 116-127.

Baker G. 1960. Fossil opal phytoliths. *Micropaleontology* **6(1)**: 79-85.

Ball TB, Brotherson JD, Gardner JS. 1993. A typologic and morphometric study of variation in phytoliths from einkorn wheat (*Triticum monococcum*). *Canadian Journal of Botany* **71(9)**: 1182-1192.

Ball TB, Gardner JS, Brotherson JD. 1996. Identifying phytoliths produced by the inflorescence bracts of three species of wheat (*Triticium monococcum* L., *T. dicoccum* Schrank and *T. aestivum* L.) using computer assisted image and statistical analyses. *Journal of Archaeological Science* **23**: 619-632.

Ball TB, Gardner JS, Anderson N. 1999. Identifying inflorescence phytoliths from selected species of wheat (*Triticum monococcum, T. dicoccon, T. dicoccoides*, and *T. aestivum*) and barley (*Hordeum vulgare* and *H. spontaneum*) (Gramineae). *American Journal of Botany* **86(11)**: 1615-1623.

Ball TB, Ehlers R, Standing MD. 2009. Review of typologic and morphometric analysis of phytoliths produced by wheat and barley. *Breeding Science* **59**: 505- 512.

Ball TB, Davis AL, Evett RR, Ladwig JL, Tromp M, Out WA, Portillo M. 2016. Morphometric analysis of phytoliths: recommendations towards standardization from the International Committee for Phytolith Morphometrics. *Journal of Archaeological Science* **68**: 106-111.

Ball T, Vrydaghs L, Mercer T, *et al.* 2017. A morphometric study of variance in articulated dendritic phytolith wave lobes within selected species of Triticeae and Aveneae. *Vegetation History and Archaeobotany* **26**: 85-97.

Barboni D, Bonnefille R, Alexandre A, Meunier J-D. 1999. Phytoliths as paleoenvironmental indicators, West Side Middle Awash Valley, Ethiopia. *Palaeogeography, Palaeoclimatology, Palaeoecology* **152**: 87-100.

Barboni D, Bremond L, Bonnefille R. 2007. Comparative studies of modern phytolith assemblages from inter-tropical Africa. *Paleogeography, Palaeoclimatology, Palaeoecology* **246**: 454-470.

Barboni D, Bremond L. 2009. Phytoliths of East African grasses: An assessment of their environmental and taxonomic significance based on floristic data. *Review of Palaeobotany and Palynology* **158**: 29-41.

Barboni D, Ashley, GM, Dominguez-Rodrigo M, Bunn H, Mabulla AZP, Baquedano E. 2010. Phytoliths infer locally dense and heterogeneus paleovegetation at FLK N and surrounding localities during upper Bed I time, Olduvai Gorge, Tanzania. *Quaternary Research* **74:** 344-354.

Barthlott W, Martens B. 1979. *Cuticulartaxonomie der Gräser eines westafrikanischen Savannengebietes unter dem Aspekt der Futterpräferenzanalyse wildlebender Großsäuger.* Tropische und Subtropische Pflanzenwelt 30, Mainz, Germany: Akademie der Wissenschaften und der Literatur, Mathematisch Naturwissenschaftliche Klasse.

Berlin AM, Ball TB, Thompson R, Herbert SC. 2003. Ptolemaic Agriculture, "Syrian Wheat", and *Triticum aestivum*. *Journal of Archaeological Science* **30**: 115-121.

Bertoldi de Pomar H. 1971. Ensayo de clasificacion morfologica de los silicofitolitos. *Ameghiniana* **8(3-4)**: 317-328.

Bertoldi de Pomar, H. 1975. Los silicofitolitos: Sinópsis de su conocimiento. *Darwiniana* **19(2-4)**:1 73206.

Blackman, E. 1971. Opaline silica in the range grasses of southern Alberta. *Canadian Journal of Botany* **49**: 769-781.

Blinnikov M, Busacca A, Whitlock C. 2002. Reconstruction of the late Pleistocene grassland of the Columbia basin, Washington, USA, based on phytolith records in loess. *Palaeogeography, Palaeoclimatology, Palaecology* **177:** 77-101.

Blinnikov MS. 2005. Phytoliths in plants and soils of the interior Pacific Northwest, USA. *Review of Palaeobotany and Palynology* **135**: 71-98.

Boury-Esnault N, Rützler K. 1997. *Thesaurus of sponge morphology*. Smithsonian Contributions to Zoology 596. Washington, D.C.: Smithsonian Institution Press.

Bozarth S. 1992. Classification of opal phytoliths formed in selected dicotyledons native to the Great Plains. In: Rapp G Jr, Mullholland SC, eds. *Phytolith systematics: Emerging issues*. New York: Plenum, 193-214.

Bozarth SR. 1993. Biosilicate assemblages of boreal forests and aspen parklands. In: Pearsall DM, Piperno DR, eds. *Current research in phytolith analysis: Applications in archaeology and paleoecology*. MASCA Research Papers in Science and Archaeology 10. University Museum of Archaeology and Anthropology, Philadelphia: University of Pennsylvania, 95-105.

Bremond L, Alexandre A, Hély C, Guiot J. 2005. A phytolith index as a proxy of tree cover density in tropical areas: calibration with leaf area index along a forest-savanna transect in south-eastern Cameroon. *Global and Planetary Change* **45**: 277-293.

Bremond, L, Alexandre A, Peyron D, Guiot J. 2008. Definition of grassland biomes from phytoliths in West Africa. *Journal of Biogeography* **35**: 2039-2048.

Bremond L, Bodin SC, Bentaleb I, Favier C, Canal S. 2017. Past tree cover of the Congo Basin recovered by phytoliths and δ^{13} C along soil profiles. *Quaternary International* **434**: 91-101.

Brown DA. 1984. Prospects and limits of a phytolith key for grasses in the Central United States. *Journal of Archaeological Science* **11**: 221-243.

Calegari MR, Lopes Paisani SD, Cecchet FA, *et al.* 2017. Phytolith signature on the Araucarias Plateau Vegetation change evidence in Late Quaternary (South Brasil). *Quaternary International* **434**: 117-128.

Carlquist S. 1996. Wood, bark, and stem anatomy of Gnetales: a summary. *International Journal of Plant Sciences* **157(S6)**:S58-S76.

Carnelli AL, Theurillat J-P, Madella M. 2004. Phytolith type frequencies in subalpine-alpine plant species of the European Alps. *Review of Palaeobotany and Palynology* **129**: 39-65.

Chávez SJ, Thompson RG. 2006. Early Maize on the Copacabana Peninsula: Implications for the Archaeology of the Lake Titicaca Basin. In: Staller JE, Tykot RH, Benz BF, eds. *Histories of maize: Multidisciplinary approaches to the prehistory, linguistics, biogeography, domestication, and evolution of maize.* Walnut Creek, CA: Left Coast Press, 415-428.

Chauhan DK, Tripathi DK, Kumar D, Kumar Y. 2011. Diversity, distribution and frequency based attributes of phytolith in *Arundo donax* L. *International Journal of Innovation in Biological and Chemical Science* **1**: 22-27.

Colliot G, Anderson PC, Bonnet N. 1997. Preliminary classification of phytolith shapes using computerized image analysis and pattern recognition. In: Pinilla A, JuanTresseras J, Machado MJ, eds. *First European Meeting on Phytolith Research. Centro de Ciencias Medioambientales,* Madrid: CSIC, Monografias 4, 275-288.

Collura LV, Neumann K. 2017. Wood and bark phytoltihs of West African woody plants. *Quaternary International* **434**: 142-159.

Cummings LS 1998. A review of recent pollen and phytolith studies from various contexts on Easter Island. In: Stevenson CM, ed. *Easter Island in Pacific Context. South Seas Symposium: The Easter Island Foundation Occasional Papers*. Los Osos, CA: Easter Island Foundation, Vol. 4: 100-106.

Dal Corso M, Nicosia C, Balista C, *et al.* 2017. Bronze Age crop processing evidence in the phytolith assemblages from the ditch and fen around Fondo Paviani, northern Italy. *Vegetation History and Archaeobotany* **26:** 5-24.

Devos Y, Vrydaghs L, Degraeve A, Fechner K. 2009. An archaeopedological and phytolitarian study of the "Dark Earth" on the site of Rue de Dinant (Brussels, Belgium). *Catena* **78**: 270-284.

Devos Y, Nicosia C, Vrydaghs L, Modrie S. 2013. Studying urban stratigraphy: Dark Earth and a microstratified sequence on the site of the Court of Hoogstraeten (Brussels, Belgium). Integrating archaeopedology and phytolith analysis. *Quaternary International* **315**: 147-166.

Dickau R, Bruno MC, Iriarte J, *et al.* 2012. Diversity of cultivars and other plant resources used at habitation sites in the Llanos de Mojos, Beni, Bolivia: Evidence from macrobotanical remains, starch grains, and phytoliths. *Journal of Archaeological Science* **39**: 357-370.

Esau K. 1965. *Plant anatomy.* 2nd ed. New York: Wiley.

Fahmy AG. 2008. Diversity of lobate phytoliths in grass leaves from the Sahel region, West Tropical Africa: Tribe Paniceae. *Plant Systematics and Evolution* **270**: 1-23.

Fernandez Honaine M, Zucol AF, Osterrieth ML. 2006. Phytolith assemblages and systematic associations in grassland species of the South Eastern Pampean Plains, Argentina. *Annals of Botany* **98**: 1155-1165.

Fernandez Honaine M, Osterrieth ML, Zucol AF. 2009. Plant communities and soil phytolith assemblages relationship in native grasslands from southeastern Buenos Aires province, Argentina. *Catena* **76**: 89-96.

Fisher EC, Albert RM, Botha G, Cawthra HC, Esteban I, Harris J, Jacobs Z, Jerardino A, Marean C, Neumann FH, Pargeter J, Poupart M, Venter J, 2013. Archaeological Reconnaissance for Middle Stone Age Sites Along the Pondoland Coast, South Africa. *T. Paleoanthropology*, 104-137.

Fredlund G, Tieszen L. 1994. Modern phytolith assemblages from the North American Great Plains. *Journal of Biogeography* **21**: 321-335.

Fujiwara H. 1993. Research into the history of rice cultivation using plant opal analysis. In: *Current research in phytolith analysis: Applications in archaeology and paleoecology. MASCA Research Papers in Science and Archaeology 10.* University Museum of Archaeology and Anthropology, Philadelphia: University of Pennsylvania, 147-158.

Gallego L, Distel RA. 2004. Phytolith assemblages in grasses native to central Argentina. *Annals of Botany* **94**: 865-874.

García-Granero JJ, Lancelotti C, Madella M. 2017. A methodological approach to the study of microbotanical remains from grinding stones: a case study in northern Gujarat (India). *Vegetation History and Archaeobotany* **26**: 43-57.

Garnier A, Neumann K, Eichhorn B, Lespez L. 2012. Phytolith taphonomy in the middle- to late-Holocene fluvial sediments of Ounjougou (Mali, West Africa). *The Holocene* **23(3)**: 416-431**.**

Geis JW. 1973. Biogenic silica in selected species of deciduous angiosperms. *Soil Science* **116**: 113-130.

Geis JW. 1978. Biogenic opal in three species of Gramineae. *Annals of Botany* **42**: 1119-1129.

Gomes Coe HH, Medina Ramos YB, Pereira dos Santos C, Carvalho da Silva AL, Pereira Silvestre C, Borrelli N, Olivera Furtado de Sousa L. 2017. Dynamics of production and accumulation of phytolith assemblages in the Restinga of Maricá, Rio de Janeiro, Brazil. *Quaternary International* **434**: 58-69.

Grass Phylogeny Working Group II: Aliscioni S, Bell HL, Besnard G, Christin PA, Columbus JT, Duvall MR, Edwards EJ, Giussani L, Hasenstab-Lehman K, Hilu KW, *et al.* 2012. New grass phylogeny resolves deep evolutionary relationships and discovers C_4 origins. *New Phytologist* **193(2)**: 304-312.

Gu Y, Zhao Z, Pearsall DM 2013. Phytolith morphology research on wild and domesticated rice species in East Asia. *Quaternary International* **287**: 141-148.

Hayward DM, Parry DW. 1975. Scanning electron microscopy of silica deposition in the leaves of barley (*Hordeum sativum* L.). *Annals of Botany* **39**: 1003-1009.

Hayward DM, Parry DW. 1980. Scanning electron microscopy of silica deposits in the culms, floral bracts and awns of barley (*Hordeum sativum* Jess.). *Annals of Botany* **46**: 541-548.

Helbaek H. 1960. Cereals and weed grasses in phase A. In: Braidwood RJ, Braidwood LS, eds. *Excavations in the Plain of Antioch I*. University of Chicago, Oriental Institute Publications 61, Appendix Il. Chicago: University of Chicago Press, 540-543.

Hodson MJ, Sangster AG. 1988. Silica deposition in the inflorescence bracts of wheat (*Triticum aestivum*). I. Scanning electron microscopy and light microscopy. *Canadian Journal of Botany* **66**: 829-838.

Hodson MJ, Westerman J, Tubb HJ. 2001. The use of inflorescence phytoliths from the Triticeae in food science. In: Meunier JD, Colin F, eds. *Phytoliths: Applications in Earth Science and Human History*. Lisse, The Netherlands: A.A. Balkema, 87-99.

Huan X, Lu H, Wang C, Tang X, Zuo X, Ge Y, He, K. 2015. Bulliform Phytolith Research in Wild and Domesticated Rice Paddy Soil in South China. PLoS ONE **10(10):** e0141255. doi:10.1371/journal. pone.0141255. http://dx.doi.org/10.1371/journal.pone.0141255.

Ishida S, Parker AG, Kennet D, Hodson MJ. 2003. Phytolith analysis from the archaeological site of Kush, Ras alKhaimah, United Arab Emirates. *Quaternary Research* **59**: 310-321.

Issaharou-Matchi I, Barboni D, Meunier JD, Saadou M, Dussouillez P, Contoux C, Zirihi-Guede N. 2016. Intraspecific biogenic silica variations in the grass species *Pennisetum pedicellatum* along an evapotranspiration gradient in South Niger. *Flora* **220**: 84-93.

Jattisha PI, Sabu M. 2012. Phytoliths as a tool for the identification of some Chloridoideae grasses in Kerala. *International Scholarly Research Network Botany*. doi 10.5402/2012/246057.

Kaplan L, Smith MB, Sneddon LA. 1992. Cereal grain phytoliths of Southwest Asia and Europe. In: Rapp G Jr. and Mulholland SC, eds. *Phytolith Systematics. Emerging Issues, Advances in Archaeological and Museum Science*. New York: Plenum Press, 149-174.

Kaufman PB, LaCroix JD, Rosen JJ, Allard LF, Bigelow WC. 1972. Scanning electron microscopy and electron microprobe analysis of silicification patterns in inflorescence bracts of *Avena sativa*. *American Journal of Botany* **59(10)**: 1018- 1025.

Kerns BK. 2001. Diagnostic phytoliths for a Ponderosa pine-bunchgrass community near Flagstaff, Arizona. *The Southwestern Naturalist* **46(3)**:282-294.

Klein RL, Geis JW. 1978. Biogenic silica in the Pinaceae. *Soil Science* **126**: 145-156.

Kondo R, Peason T. 1981. Opal phytoliths in trees leaves (part 2): opal phytoliths in dicotyledon angiosperm tree leaves. *Research Bulletin of Obihiro University* **12**: 217-229. In Japanese, with English abstract.

Kondo R, Childs C, Atkinson I. 1994. *Opal phytoliths of New Zealand.* Lincoln, New Zealand: Manaaki Press.

Lu HY, Liu KB. 2003. Phytoliths of common grasses in the coastal environments of southeastern USA. *Estuarine Coastal and Shelf Science* **58**: 587-600.

Lu HY, Zhang JP, Wu NQ, Liu KB, Xu D, Li Q. 2009. Phytoliths analysis for the discrimination of foxtail millet (*Setaria italica*) and common millet (*Panicum miliaceum*). *Plos One* **4(2)**: e4448.

Madella M, Jones MK, Goldberg P, Goren Y, Hovers E. 2002. The exploitation of plant resources by Neanderthals in Amud Cave (Israel): The evidence from phytolith studies. *Journal of Archaeological Science* **29**: 703-719.

Madella M, Alexandre A, Ball T. 2005. International Code for Phytolith Nomenclature 1.0. *Annals of Botany* **96:** 253-260.

Madella M, Garcia-Granero JJ, Out WA, Ryan P, Usai D. 2014. Microbotanical evidence of domestic cereals in Africa 7000 years ago. *Plos One* **9(10)**: e110177.

Madella M, Lancelotti C, Garcia-Granero JJ. 2016. Millet microremains – an alternative approach to understand cultivation and use of critical crops in prehistory. *Archaeological and Anthropological Sciences* 8: 17-28.

Mazumdar J. 2011. Phytoliths of pteridophytes. *South African Journal of Botany* **77**: 10-19.

Meister J, Krause J, Müller-Neuhof B, Portillo M, Reimann T, Schütt B. 2017. Desert agricultural systems at EBA Jawa (Jordan): integrating archaeological and paleoenvironmental records. *Quaternary International* **434:** 43-50.

Mercader J, Bennett T, Esselmont C, Simpson S., Walde D. 2009. Phytoliths in woody plants from the Miombo woodlands of Mozambique. *Annals of Botany* **104**: 91-113.

Mercader J, Astudillo F, Barkworth M, Bennett T, Esselmont C, Kinyanjui R, Grossman DL, Simpson S, Walde D. 2010. Poaceae phytoliths from the Niassa Rift, Mozambique. *Journal of Archaeological Science* **37:** 1953-1967.

Mercader J, Bennett T, Esselmont C, Simpson S, Walde D. 2011. Soil phytoliths from miombo woodlands in Mozambique. *Quaternary Research* **75**: 138-150.

Metcalfe CR. 1960. Anatomy of the Monocotyledons, Iineae. London: Oxford Univ. Press.

Metcalfe CR. 1971. Anatomy of the monocotyledons, Cyperaceae, v.5. Oxford: Clarendon Press.

Morcote-Rios G, Giraldo-Canas D, Raz L. 2015. *Catálogo ilustrado de fitolitosc ontemporá-neos con énfasis arqueológico y paleoecológico I. Gramineas amazonicas de Colombia.* Bogotá, Colombia: Biblioteca José Jerónimo Triana 31, Universidad Nacional de Colombia, Facultad de Ciencias, Instituto de Ciencias Naturales, Sede Bogotá.

Morris LR, Baker FA, Morris C, Ryel RJ. 2009. Phytolith types and type frequencies in native and introduced species of the sagebrush steppe and pinyon juniper woodlands of the Great Basin, USA. *Review of Palaeobotany and Palynology* **157**: 339-357.

Mulholland SC. 1989. Phytolith shape frequencies in North Dakota grasses: A comparison to general patterns. *Journal of Archaeological Science* **16**: 489-511.

Mulholland SC, Rapp G Jr. 1992. A morphological classification of grass silica- bodies. In: Rapp G Jr, Mulholland SC, eds. *Phytolith Systematics. Emerging Issues, Advances in Archaeological and Museum Science*. New York: Plenum Press, 65-89.

Naskar M, Bera S. 2018. Taxonomic assessment of opal phytoliths from grasses of deltaic West Bengal; India. *Nordic Journal of Botany* **36(4)**: 1-42.

Neumann K, Fahmy AG, Müller-Scheeßel N, Schmidt M. 2017. Taxonomic, ecological and palaeoecological significance of leaf phytoliths in West African grasses. *Quaternary International* **434**: 15-32.

Novello A, Barboni D, Berti-Equille L, Mazur JC, Poilecot P, Vignaud P. 2012. Phytolith signal of aquatic plants and soils in Chad, Central Africa. *Review of Palaeobotany and Palynology* **178**: 43-58.

Novello A, Barboni D. 2015. Grass inflorescence phytoliths of useful species and wild cereals from sub-Saharan Africa. *Journal of Archaeological Science* **59**: 10-22.

Ollendorf AL. 1992. Towards a classification scheme of sedge (Cyperaceae) phytoliths. In: Rapp G Jr, Mulholland SC, eds. *Phytolith systematics. Emerging issues.* New York: Plenum, 91-106.

Palmer PG, Gerbeth-Jones S. 1986. A scanning electron microscope survey of the epidermis of East African grasses, IV. Washington D.C.: Smithsonian Contributions to Botany 62. Smithsonian Institution Press.

Palmer PG, Gerbeth-Jones S. 1988. A scanning electron microscope survey of the epidermis of East African grasses, V, and West African supplement. Smithsonian Contributions to Botany 67. Smithsonian Institution Press.

Palmer PG, Tucker AE. 1981. A scanning electron microscope survey of the epidermis of East African grasses, I. Washington D.C.: Smithsonian Contributions to Botany 49. Smithsonian Institution Press.

Palmer PG, Tucker AE. 1983. A scanning electron microscope survey of the epidermis of East African grasses, II. Washington D.C.: Smithsonian Contributions to Botany 53. Smithsonian Institution Press.

Palmer PG, Gerbeth-Jones S, Hutchison S. 1985. A scanning electron microscope survey of the epidermis of East African grasses, III. Washington D.C.: Smithsonian Contributions to Botany 55. Smithsonian Institution Press.

Parry DW, Smithson F. 1964. Types of opaline silica depositions in the leaves of British grasses. *Annals of Botany* **28(109)**: 169-185.

Parry DW, Smithson F. 1966. Opaline silica in the inflorescences of some British grasses and cereals. *Annals of Botany* **30(119)**: 524-538.

Pearsall DM. 1978. Phytolith analysis of archeological soils: Evidence for maize cultivation in Formative Ecuador. *Science* **199(4325)**: 177-178.

Pearsall DM. 1982. Phytolith analysis: Applications of a new paleoethnobotanical technique in archaeology. *American Anthropologist* **84(4)**: 862-871.

Pearsall DM, Dinan EH. 1992. Developing a phytolith classification system. In: Rapp G Jr, Mulholland SC, eds. *Phytolith systematics. Emerging issues.* New York: Plenum, 37-64.

Pearsall DM, Piperno DR, Dinan EH, Umlauf R, Zhao ZJ, Benfer RA. 1995. Distinguishing rice (Oryza-Sativa Poaceae) from wild Oryza species through phytolith analysis - results of preliminary research. *Economic Botany* **49**: 183-196.

Pető Á, Gyulai F, Popity D, Kenez A. 2013. Macro and microarchaeobotanical study of a vessel content from a Late Neolithic structured deposition from southeastern Hungary. *Journal of Archaeological Science* **40(1)**: 58-71.

Phillips C, Lancelotti C. 2014. Chimpanzee diet: phytolithic analysis of feces. *American Journal of Primatology* **76(8)**: 757-773.

PhytCore DB - Phytolith online database. 2016.
http://www.phytcore.org/phytolith/index.php?rdm=Lz8crv6ynr&action=searchphyt

Piperno, DR. 1983. *The application of phytolith analysis to the reconstruction of plant subsistence and environments in prehistoric Panama*. PhD Dissertation, Temple University, Philadelphia, PA.

Piperno DR. 1984. A comparison and differentiation of phytoliths from maize (*Zea mays* L.) and wild grasses: Use of morphological criteria. *American Antiquity* **49(2)**: 361-383.

Piperno DR. 1988. *Phytolith analysis: an archaeological and geological perspective.* San Diego: Academic Press.

Piperno, DR, Pearsall DM. **1998**. *The silica bodies of tropical American grasses: Morphology, taxonomy, and implications for grass systematics and fossil phytolith identification*. Washington D.C.: Smithsonian Contributions to Botany 85. Smithsonian Institution Press.

Piperno DR. 2006. *Phytoliths. A comprehensive guide for archaeologists and palaeoecologists.* Lanham: AltaMira Press.

Piperno DR. 2009. Identifying crop plants with phytoliths (and starch grains) in Central and South America: A review and an update of the evidence. *Quaternary International* **193**: 146-159.

Piperno DR, Ranere AJ, Holst I, Iriarte J, Dickau R. 2009. Starch grain and phytolith evidence for early ninth millennium BP maize from the Central Balsas River Valley, Mexico. *Proceedings of the National Academy of Sciences of the United States of America* **106**: 5019-5024.

Portillo M, Valenzuela S, Albert RM. 2012. Domestic patterns in the Numidian site of Althiburos (northern Tunisia): The results from a combined study of animal bones, dung and plant remains. *Quaternary International* **275**: 84-96.

Postek MT. 1981. The occurrence of silica in the leaves of *Magnolia grandiflora* L. *Botanical Gazette* **142(1)**: 124-134.

Power RC, Rosen AM, Nadel D. 2014. The economic and ritual utilization of plants at the Raqefet Cave Natufian site: The evidence from phytoliths. *Journal of Anthropological Archaeology* **33**: 49-65.

Prasad V, Stromberg CAE, Alimohammadian H, Sahni A. 2005. Dinosaur coprolites and the early evolution of grasses and grazers. *Science* **310**: 1177-1180.

Prasad V, Stromberg CAE, Leache D, *et al.* 2011. Late Cretaceous origin of the rice tribe provides evidence for the early diversification in Poaceae. *Nature Communications* **2**: 480.

Prat H. 1948. General features of the epidermis in Zea mays. *Annals of the Missouri Botanical Garden* **35**: 341-351.

Radomski, KU, Neumann, K. 2011. Grasses and grinding stones: Inflorescence phytoliths from modern West African Poaceae and archaeological stone artefact. In Fahmy A, Kahlheber S, D'Andrea AC, eds. *Windows on the African Past. Current Approaches to African Archaeobotany*. Frankfurt am Main: Africa Magna, 153-164.

Raigemborn M, Brea M, Zucol A, Matheos S. 2009. Early Paleogene climate at mid latitude in South America: Mineralogical and paleobotanical proxies from continental sequences in Golfo San Jorge basin (Patagonia, Argentina). *Geologica Acta* **7(1-2)**: 125-145. DOI: 10.1344/105.000000269.

Rosen AM. 1992. Preliminary identification of silica skeletons from Near Eastern archaeological sites: An anatomical approach. In: Rapp G Jr, Mulholland SC, eds. *Phytolith systematics. Emerging issues.* New York: Plenum, 129-147.

Rosen AM, Weiner S. 1994. Identifying ancient irrigation: a new method using opaline phytoliths from emmer wheat. *Journal of Archaeological Science* **21**: 125-132.

Rosen, AM 2001. Phytolith evidence for agropastoral economies in the Scythian period of southern Kazakhstan. In: Meunier, JD and Colin F eds, *Phytoliths: Applications in Earth Science and Human History*. Lisse, The Netherlands: A.A. Balkema, 183-198.

Rovner I. 1983. Phytolith analysis. In: Turnbow C, Jobe C, O'Malley N, eds. *Archaeological excavation of the Goolman, DeVary and Stone sites in Clark County, Kentucky. Archaeology Report N° 78:269279*. Lexington, KY: University of Kentucky, 269-279.

Rudall, PJ, Prychid CJ, Gregory T. 2014. Epidermal patterning and silica phytoliths in grasses: an evolutionary history. *The Botanical Review* **80**: 59-71,

Runge F 1998. *Opalphytolithe in den Tropen Afrikas und ihre Verwendung bei der Rekonstruktion paläoökologischer Umweltverhältnisse.* Habilitation thesis. University of Paderborn, Paderborn, Germany.

Runge F. 1999. The opal phytolith inventory of soils in central Africa - quantities, shapes, classification and spectra. *Review of Palaeobotany and Palynology* **107**: 23-53.

Sangster AG, Parry DW. 1969. Some factors in relation to bulliform cell silicification in the grass leaf. *Annals of Botany* **33:** 315-323.

Sangster AG, Hodson MJ, Parry DW, Rees JA. 1983. A developmental study of silicification in the trichomes and associated epidermal structures of the inflorescence bracts of the grass *Phalaris canariensis* L. *Annals of Botany* **52**: 171-187.

Sangster AG, Williams SE, Hodson MJ . 1997. Silica deposition in the needles of the gymnosperms. II. Scanning electron microscopy and xray microanalysis. In: Pinilla A, Juan-Tresseras J, Machado MJ, eds. *First European Meeting on Phytolith Research. Centro de Ciencias Medioambientales,* Madrid: CSIC, Monografias 4, 135-146.

Sase T, Hosono M. 2001. Phytolith record in soils interstratified with late quaternary tephras overlying the Eastern región of Towada volcano, Japan. In: Meunier JD, Colin F, eds. *Phytoliths: Applications in Earth Science and Human History*. Lisse, The Netherlands: A.A. Balkema, 57-71.

Schneider EL, Carlquist S. 1999. SEM studies on vessels in ferns. 11. Ophioglossum. *Botanical Journal of the Linnean Society* **129(2)**:105-114.

Scurfield G, Anderson CA, Segnit ER. 1974. Silica in woody stems. *Australian Journal of Botany* **22**: 29-211.

Shillito LM. 2011. Taphonomic observations of archaeological wheat phytoliths from Neolithic Catalhoyuk, Turkey, and the use of conjoined phytolith size as an indicator of water availability. *Archaeometry* **53**: 631-641.

Soreng RJ, Peterson PM, Romaschenko K, Davidse G, Zuloaga FO, Judziewicz EJ, Filgueiras TS, Davis JI, Morrone O. 2015. A worldwide phylogenetic classification of the Poaceae (Gramineae). *Journal of Systematics and Evolution* **53(2)**: 117-137.

Strömberg CAE. 2003. *The origin and spread of grass-dominated ecosystems during the Tertiary of North America and how it relates to the evolution of hypsodonty in Equids.* PhD thesis, University of California, Berkeley, USA.

Strömberg CAE. 2004. Using phytolith assemblages to reconstruct the origin and spread of grass-dominated habitats in the Great Plains during the late Holocene to early Miocene. *Palaeogeography, Palaeoclimatology, Palaeoecology* **207**: 239-275.

Stromberg, CAE. 2005. Decoupled taxonomic radiation and ecological expansion of open-habitat grasses in the Cenozoic of North America. *Proceedings of the National Academy of Sciences of the United States of America* **102**: 11980-11984.

Strömberg CAE, Werdelin L, Friis EM, Saraç G. 2007. The spread of grass-dominated habitats in Turkey and surrounding areas during the Cenozoic: phytolith evidence. *Palaeogeography, Palaeoclimatology, Palaeoecology* **250 (1-4)**: 18-49.

Strömberg CAE, Dunn RE, Madden RH, Kohn MJ, Carlini AA. 2013. Decoupling the spread of grasslands from the evolution of grazer-type herbivores in South America. *Nature Communications* DOI: 10.1038/ncomms2508

Thorn VC. 2004. *An annotated bibliography of phytolith analysis and atlas of selected New Zealand subantartic and subalpine phytoliths.* Wellington, New Zealand: Antarctic Data Series 29. Antarctic Research Centre, Victoria University of Wellington.

Tubb HJ, Hodson MJ, Hodson GC. 1993. The inflorescence papillae of the Triticeae: A new tool for taxonomic and archaeological research. *Annals of Botany* **72**: 537-545.

Tsartsidou G., Lev-Yadun S., Albert RM, Miller-Rosen A., Efstratiou N, Weiner S. 2007. The Phytolith Archaeological Record: Strengths and Weaknesses Based on a Quantitative Modern Reference Collection from Greece. *Journal of Archaeological Science* **34 (8):** 1262-1275.

Twiss PC, Suess E, Smith RM. 1969. Morphological classification of grass phytoliths. *American Society for Soil Science, Proceedings* **33(1)**: 109-115.

Twiss PC. 1992. Predicted world distribution of C3 and C4 grass phytoliths. In: Rapp G Jr, Mulholland SC, eds. *Phytolith systematics. Emerging issues*. New York: Plenum, 113--128.

Vrydaghs L, Ball TB, Devos Y. 2016. Beyond redundancy and multiplicity. Integrating phytolith analysis and micromorphology to the study of Brussels Dark Earth. *Journal of Archaeological Science* **68**: 79-88.

Wallis LA. 2003. An overview of leaf phytolith production patterns in selected northwest Australian flora. *Review of Palaeobotany and Palynology* **125**: 201-248.

Wang JJ, Liu L, Ball TB, Yu LJ, Li YQ, Xing FL. 2016. Revealing a 5,000-y-old beer recipe in China. *Proceedings of the National Academy of Sciences of the United States of America* **113(23)**: 6444-6448.

Watson L, Dallwitz MJ. 1992 onwards. Grass genera of the world: Descriptions, illustrations, identification, and information retrieval; including synonyms, morphology, anatomy, physiology, phytochemistry, cytology, classification, pathogens, world and local distribution, and references. Version: 23rd April 2010. http://delta-intkey.com/.

Yost CL, Blinnikov MS. 2011. Locally diagnostic phytoliths of wild rice (*Zizania palustris L*.) from Minnesota, USA: comparison to other wetland grasses and usefulness for archaeobotany and paleoecological reconstructions. *Journal of Archaeological Science* **38**: 1977-1991.

Yost CL, Jackson LJ, Stone JR, Cohen AS. 2018. Subdecadal phytolith and charcoal records from Lake Malawi, East Africa imply minimal effects on human evolution from the ~74 ka Toba supereruption. *Journal of Human Evolution* **116**: 75-94.

Zhang JP, Lu HY, Wu NQ, Qin XG, Wang L. 2013. Palaeoenvironment and agriculture of ancient Loulan and Milan on the Silk Road. *Holocene* **23(2)**: 208- 217.

Zucol AF, Brea M, Bellosi ES. 2008. Phytolith studies in Gran Barranca (central Patagonia, Argentina): The middle-late Eocene. In: Madden RH, Carlini AA, Vucetich MG, Kay RF eds. *The Paleontology of Gran Barranca – Evolution and Environmental Change through the Middle Cenozoic of Patagonia*. Cambridge: Cambridge University Press, 317-340.